coatings

MDPI

Review

Advances in Charge Carrier Mobility of Diketopyrrolopyrrole-Based Organic Semiconductors

Zhengran He [1,*], Kyeiwaa Asare-Yeboah [1] and Sheng Bi [2,*]

[1] Department of Electrical and Computer Engineering, Penn State University Behrend, Erie, PA 16563, USA
[2] Key Laboratory for Precision and Non-Traditional Machining Technology of the Ministry of Education, Dalian University of Technology, Dalian 116024, China
* Correspondence: zmh5222@psu.edu (Z.H.); bish@dlut.edu.cn (S.B.)

Abstract: In recent years, the charge carrier mobility study of organic semiconductors has seen significant progress and surpassed that of amorphous silicon thanks to the development of various molecular engineering, solution processing, and external alignment methods. These advances have allowed the implementation of organic semiconductors for fabricating high-performance organic electronic devices. In particular, diketopyrrolopyrrole-based small-molecular and polymeric organic semiconductors have garnered considerable research interest due to their ambipolar charge-carrier properties. In this article, we focus on conducting a comprehensive review of previous studies that are dedicated to the external alignment, thermal annealing, and molecular engineering of diketopyrrolopyrrole molecular structures and side-chain structures in order to achieve oriented crystal orientation, optimized thin-film morphology, and enhanced charge carrier transport. By discussing these benchmark studies, this work aims to provide general insights into optimizing other high-mobility, solution-processed organic semiconductors and sheds lights on realizing the acceleration of organic electronic device applications.

Keywords: diketopyrrolopyrrole; mobility; organic semiconductor; organic thin-film transistors; organic electronics

Citation: He, Z.; Asare-Yeboah, K.; Bi, S. Advances in Charge Carrier Mobility of Diketopyrrolopyrrole-Based Organic Semiconductors. *Coatings* **2024**, *14*, 1080. https://doi.org/10.3390/coatings14091080

Academic Editor: Aomar Hadjadj

Received: 19 July 2024
Revised: 15 August 2024
Accepted: 21 August 2024
Published: 23 August 2024

1. Background and Challenges

1.1. Advances in Charge Carrier Mobilities

In recent years, research in the charge carrier transport of solution-processed organic semiconductors has advanced at an exponential rate, allowing the mobilities to facilely surpass those of amorphous silicon [1–8]. For example, Tazuhara and colleagues documented the growth of 2,7-didodecyl[1]benzothieno[3,2-b][1]benzothiophene (C_{12}-BTBT) organic crystals with extensive polycrystalline domains using a binary toluene/mesitylene solvent approach, which generated a mobility of 10 cm^2/Vs [9]. Tripathi et al. reported the ambipolar charge transport in a 9,10-diphenylanthracene (DPA) organic semiconductor, which comprises phenyl groups at the anthracene backbone positions [10]. The DPA bulk crystals showed an electron mobility of 13 cm^2/Vs, as well as a lower hole mobility of 3.7 cm^2/Vs, which at a high-temperature regime featured bandlike transport behavior. Xue et al. reported a method of removing polar solvent residues in order to enhance the mobility of 6,13-bis(triisopropylsilylethynyl)-5,7,12,14-tetraazapentacene (TIPS-TAP) [11]. After the polar solvent residues were removed, the TIPS-TAP crystal ribbons with an alignment of several hundred micrometers demonstrated a 60% improvement in mobility with an electron mobility of up to 13.3 cm^2/Vs. He et al. reported the solution-based self-assembly of dihexyl-substituted DBTDT (C6-DBTDT) organic crystals with two different phases [12]. Drop-casting C6-DBTDT in a concentrated chlorobenzene solution resulted in platelet-like single crystals with an α-phase, whereas a diluted solution yielded microribbon-like single crystals with a β-phase, giving rise to mobilities of 8.5 cm^2/Vs and 18.9 cm^2/Vs, respectively. Jurchescu et al. reported the incorporation of 6,13-pentacenequinone (PQ) as a gate

dielectric material to improve the single-crystal charge transport of pentacene [13]. The interface-scattering centers of the PQ dielectric layer led to a high-quality interface and yielded a hole mobility of 40 cm^2/Vs.

1.2. Advances in Organic Electronic Device Applications

The elevated charge carrier mobilities have further sparked research interest in developing high-performance organic semiconductor devices, including organic gas sensors, photodetectors, and complementary inverters. In this section, we briefly discuss those device applications in order to shed light on opening up the avenue to realizing high-efficiency flexible electronics.

Lee et al. reported the detection of ammonia gas molecules by fabricating a 6,13-bis(triisopropylsilylethynyl)pentacene (TIPS pentacene)-based gas sensor. The enhanced rate of ammonia gas adsorption to the TIPS pentacene film surface allowed the electrons to react with the semiconductor hole charge carriers and reduced the overall positive charge, giving rise to the capability of detecting an even lower gas concentration [14]. Hou et al. reported the detection of nitrogen dioxide gas by using a TIPS pentacene-based gas sensor. The enhanced density of the grain boundaries as a result of annealing TIPS pentacene with solvent vapors improved the NO_2 gas adsorption and improved the gas sensor responsivity by an order of magnitude [15]. Benavides et al. reported TIPS pentacene was demonstrated as an interlayer in a poly-3-hexyl-thiophene(P3HT)/[6, 6]-phenyl C61 butyric acid methyl ester heterojunction configuration in order to reduce the dark current of the photodetectors [16]. The insertion of the TIPS pentacene interlayer significantly enhanced the photodetector performance by elevating the device's dynamic range and increasing the photodetector detectivity of green light irradiation. Zhao et al. reported C_{60} and TIPS pentacene single crystals with both excellent electron and hole mobility were employed in fabricating highly sensitive photodetectors [17]. The absorption of C_{60} and TIPS pentacene single crystals gave rise to excellent responsivities, ranging from ultraviolet light to the near-infrared light. Jea et al. reported successive deposition of TIPS pentacene and F_{16}CuPc microarrays with alternating directional *p*-channels and *n*-channels [18]. The transistor devices fabricated by using this method revealed ambipolar charge transport characteristics, which were applied in air-stable complementary inverters. Janneck et al. reported a zone-casting method to fabricate highly crystalline 2,7-dioctyl[1]benzothieno[3,2-b][1]benzothiophene (C_8-BTBT)-based long-channel transistors with 7.5 cm^2/V mobility and integrated them into inverters [19]. The inverter device comprised a 19-stage ring oscillator and showed gains up to 40 and an operating frequency of 630 Hz.

1.3. Current Challenges in Organic Electronics

Despite these aforementioned advances, the in-solution processing of both small-molecular and polymeric organic semiconductors has met ongoing challenges, which has impeded applications in high-performance flexible electronics [20–24]. Here, we will briefly discuss each of these challenges, including nonuniform morphology, low crystallinity, and nonoptimal molecular packing [25–30]. First of all, nonuniform morphology features crystal misorientation, inferior substrate coverage, and grain-width variations. Crystal misorientation arises from drop-casting organic semiconductor solution and the substrate anisotropic crystal growth behavior [31–37]. For instance, several studies have reported that drop-casting organic semiconductors, such as TIPS pentacene and 5,6,11,12-Tetrachlorotetracene, caused the crystal to grow in anisotropic directions [38–43]. When those misoriented crystals were manipulated as the device active layer of thin-film transistors, such misoriented crystals could further induce anisotropic mobilities [44–47]. A previous report indicated that the mobilities measured from randomly aligned TIPS pentacene organic crystals can vary by one order of magnitude [48]. Such mobility variation can be further exaggerated to three to four orders of magnitude based on the different crystal coverage in the charge transport channel [49]. Those dramatic mobility variations have made it challenging to apply these organic semiconductors for fabricating high-performance organic electronic

devices. For these reasons, it becomes highly desirable to apply alignment methods to externally confine the direction in which the organic semiconductors may crystallize. Those external force alignment methods include substrate patterning-based methods [50–56], solution shearing-based methods [57–59], capillary force-based methods [60–62], and so on.

Thin films for organic semiconductors are typically produced using various techniques such as spin-coating [63–66], drop-casting [67–69], and spray-coating [70–73]. Each of these methods offers unique advantages and disadvantages depending on the desired film morphology, uniformity, and thickness control. Spin-coating is widely used for its ability to produce uniform thin films with controlled thickness, but it often results in low crystallinity due to rapid solvent evaporation. Drop-casting, on the other hand, allows for better crystallinity but can lead to nonuniform film morphology with significant variations in grain size. Spray-coating provides a scalable approach for large-area coatings, though it can be challenging to achieve uniform film thickness and high crystallinity. Table 1 summarizes the key characteristics of these methods. Consequently, post-thermal annealing or solvent annealing is typically applied to spin-coated organic semiconductor films in order to increase the crystallinity of the semiconductor film and to enhance the charge carrier mobilities [74–78].

Table 1. A list of each method typically used for depositing organic semiconductors, as well as the advantages and disadvantages of each method.

Method	Advantages	Disadvantages
Spin-Coating	Uniform film thickness, easy to control	Low crystallinity, limited to small areas
Drop-Casting	High crystallinity, simple equipment	Nonuniform morphology, grain size variation
Spray-Coating	Scalable for large areas, suitable for flexible substrates	Challenging thickness control, lower crystallinity

Table 1 lists each method used for depositing organic semiconductors discussed in this section, with their advantages and disadvantages.

Furthermore, nonoptimal molecular packing has been an issue that obstructs the electrical charge transport of organic semiconductors. Thus, side-chain engineering has become an effective method to improve the molecular packing of organic semiconductors. Various studies have reported miscellaneous molecular engineering and side-chain modifications which give rise to high-mobility organic semiconductors. For instance, miscellaneous small-molecular and polymeric organic semiconductors have been developed based on diketopyrrolopyrrole (DPP)-based material by side-chain engineering, yielding a mobility close to 10 cm^2/Vs [79–81]. Small-molecular 6,13-bis(triisopropylsilylethynyl) TIPS pentacene is an organic semiconductor developed upon its predecessor pentacene as a soluble counterpart in organic solvents [38,82]. The bulky alkyl side-chain engineering allows TIPS pentacene to interrupt the herringbone packing motif and thereby to exhibit improved solubility in organic solvents [83–85]. The enhanced π-π stacking in TIPS pentacene favors charge transport and leads to hole mobilities over 10 cm^2/Vs [86]. C_8-BTBT is an organic polymeric semiconductor incorporating the [1]benzothieno[3,2-b][1]-benzothiophene unit as the base material, which has been showcased with mobilities reaching over 40 cm^2/Vs [87].

Given the importance of these benchmark organic semiconducting small molecules and polymers, various review articles [88–96] have recently come to light that summarize the tremendous efforts dedicated to addressing these aforementioned challenges of employing TIPS pentacene and C_8-BTBT for fabricating thin-film transistors. Nevertheless, a detailed review of implementing diketopyrrolopyrrole in fabricating thin-film transistors has not been reported yet. In this article, we will conduct a comprehensive review of the various works dedicated to the solution processing, crystal growth, external alignment, molecular engineering, and charge transport properties of the diketopyrrolopyrrole-based small-molecular and polymeric organic semiconductors. In particular, we will review

these works in the categories of external alignment, thermal annealing, and molecular engineering. Figure 1 shows the molecular structures of diketopyrrolopyrrole-based small-molecular and polymeric organic semiconductors reviewed in our article. By investigating these examples, we shed light on the importance of optimizing semiconductor crystallization, film morphology, crystal alignment, and ambipolar behavior in order to maximize the charge transport property of diketopyrrolopyrrole-based organic semiconductors.

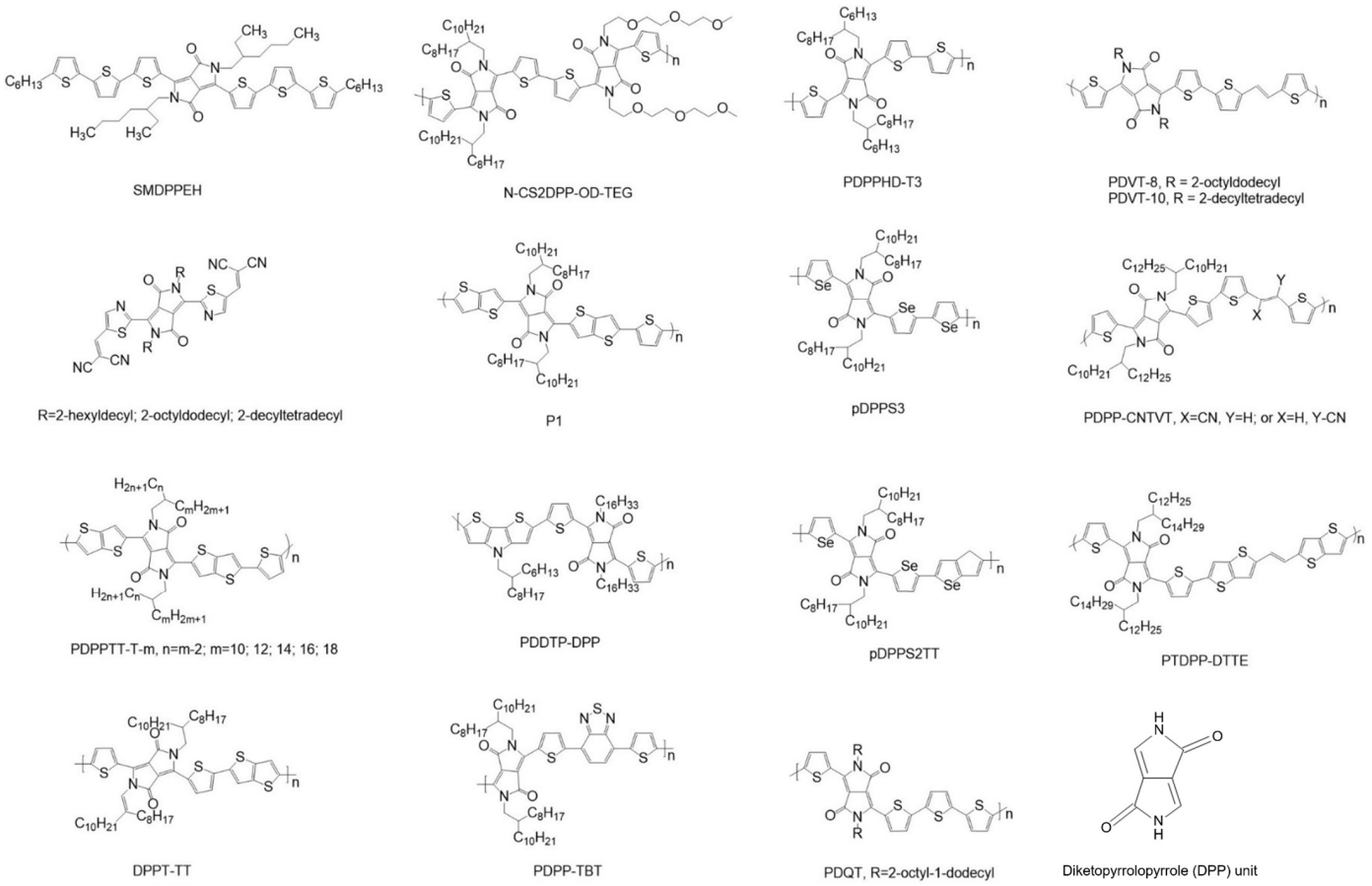

Figure 1. The molecular structures of various small-molecular and polymeric semiconductors based on diketopyrrolopyrrole that are reviewed in this article.

2. Review of Diketopyrrolopyrrole-Based Organic Semiconductors

2.1. Properties of Diketopyrrolopyrrole-Based Organic Semiconductors

Diketopyrrolopyrrole-based pigments have been reported with various colors that ranged from red to blue [97–101]. The synthesis of diketopyrrolopyrrole pigment was first reported by Parnum et al. in a pivotal study in 1974. The flanking with two phenyl units led to an insoluble hydrocarbon pentalene-based molecule with an 8-π electron-fused ring [102]. Iqbal et al. developed diketopyrrolopyrrole dyes and pigments and improved the yield by demonstrating a single reaction process between dialkyl succinate and aromatic nitrile [103]. Following these studies, diketopyrrolopyrrole derivatives with various side-chain engineering and functionalizations have been reported with more varieties of colors [80,104]. For instance, diketopyrrolopyrrole flanked with side chains exhibits modified planarity, π-π stacking distance, energy states, and charge transport properties. In particular, these properties make diketopyrrolopyrrole attractive for miscellaneous organic electronic devices, including organic sensors, solar cells, and thin-film transistors. Therefore, in diketopyrrolopyrrole-based semiconductors, π-π interactions and molecular aggregation significantly influence electron and hole mobility. The planarity of the diketopyrrolopyrrole core, facilitated by these π-π interactions, enhances charge transport by

promoting efficient stacking, which in turn decreases the π-π stacking distance [105–107]. Molecular aggregation further contributes to charge transport by increasing crystallinity and order in the film. The side-chain modifications include varying the length and branching of alkyl chains. These modifications affect the molecular packing, which quantitatively influences the π-π stacking distance and thus the charge transport properties.

Diketopyrrolopyrrole-based materials have garnered significant attention for their tunable bandgaps and energy levels, which are critical for optimizing device performance in organic field-effect transistors (OFETs) [108–113] and organic photovoltaics (OPVs) [114–118]. The bandgap of diketopyrrolopyrrole-based polymers typically ranges between 1.5 and 2.0 eV, making them suitable for absorbing visible light, a crucial characteristic for OPV applications. The energy levels, including the highest occupied molecular orbital (HOMO) and lowest unoccupied molecular orbital (LUMO), are finely tuned through side-chain engineering and donor–acceptor molecular design, enabling efficient charge separation and transport. Density functional theory (DFT) modeling has provided insights into the charge transfer mechanisms at the molecular level, revealing that the donor–acceptor interactions significantly enhance charge delocalization and mobility [101,119]. These theoretical models are crucial for understanding the molecular origins of the high-performance characteristics observed in DPP-based devices.

Additionally, the transition from laboratory-scale synthesis to pilot-scale and industrial-scale production of diketopyrrolopyrrole-based conjugated materials presents several challenges, including scalability, cost-effectiveness, and material purity. Diketopyrrolopyrrole, isoDPP, and their derivatives require precise synthetic routes that can be difficult to replicate on a larger scale [120–122]. Recent advances in continuous flow chemistry and scalable polymerization techniques have begun to address these challenges, enabling the production of high-purity diketopyrrolopyrrole-based materials with consistent properties. However, further development is needed to optimize these processes for industrial-scale production. Challenges such as the handling of reactive intermediates, the control of molecular weight distribution, and the minimization of by-products must be overcome to ensure that diketopyrrolopyrrole-based materials can be produced at scale while maintaining their high performance in electronic applications. These advancements are critical for the widespread adoption of diketopyrrolopyrrole-based materials in commercial electronics and photovoltaic devices.

Furthermore, while diketopyrrolopyrrole-based organic semiconductors have demonstrated significant advancements in charge carrier mobility and have been widely explored for applications in organic electronics, it is essential to contextualize these developments within the broader landscape of semiconductor materials. Inorganic semiconductors such as Fe_2O_3, Cu_2O, and CeO_2 have long been established in the field due to their robust thermal stability, high carrier mobility, and suitability for high-temperature applications, and they also rely on thermal treatments to stabilize their crystalline phases and optimize their electronic properties [123–126]. However, they often lack the flexibility, tunability, and solution-processability that organic materials offer. Diketopyrrolopyrrole-based materials, with their tunable electronic properties through side-chain engineering and molecular design, present unique advantages in applications requiring lightweight, flexible, and solution-processable devices. Yet, challenges such as stability, environmental impact, and manufacturability need to be addressed.

A comprehensive understanding of photon-excited charge-carrier mechanisms, photoredox processes, plasmonic effects, and dielectric properties is critical for optimizing the performance of diketopyrrolopyrrole-based materials in applications such as photodetectors and gas sensors [127–136]. When diketopyrrolopyrrole-based semiconductors absorb photons, they generate electron–hole pairs that are vital for initiating photocatalytic reactions. The efficiency of charge separation and the subsequent electron transfer to surface-adsorbed species play a significant role in determining the material's photocatalytic activity. Compared to inorganic semiconductors like Fe_2O_3, Cu_2O, and CeO_2, which are known for their strong charge carrier mobilities and stable performance [137–139],

diketopyrrolopyrrole-based materials offer the advantage of molecular tunability, which can optimize light absorption and charge carrier dynamics. However, the intrinsic stability of diketopyrrolopyrrole-based materials is a concern that must be addressed to enhance their long-term performance. Further research into hybrid organic–inorganic systems and the incorporation of plasmonic nanoparticles could unlock new opportunities to enhance the efficiency, stability, and applicability of diketopyrrolopyrrole-based semiconductors. Addressing these challenges while leveraging the strengths of diketopyrrolopyrrole-based semiconductors could pave the way for their broader application in the industry [140–142].

Bürgi et al. reported a thiophene-flanked diketopyrrolopyrrole polymer with ambipolar charge transport properties. The ambipolar transistor device showed an electron and hole mobility of 0.1 cm^2/Vs and 0.09 cm^2/Vs, respectively [143]. Diketopyrrolopyrrole pigments are usually composed of a diketopyrrolopyrrole core and flanked aromatic groups. The diketopyrrolopyrrole core has amine units and bicyclic carbonyl groups, and this can provide strong electron deficiency to the diketopyrrolopyrrole pigments. This property can be useful for donor acceptor conjugated semiconductor construction. DPP-based semiconductors showcase intensive π-π interactions and molecular aggregation, which is promising for being applied in organic electronic devices. The molecular design of thiophene-flanked DPP polymers plays a crucial role in balancing electron and hole mobilities. The incorporation of electron-deficient and electron-rich segments within the polymer backbone influences this balance. Critical factors affecting the balance include the energy level alignment, molecular packing, and film morphology. The design strategy of combining strong donor and acceptor units ensures that both types of charge carriers are effectively transported, resulting in ambipolar characteristics with balanced mobilities.

2.2. External Alignment of Diketopyrrolopyrrole-Based Organic Semiconductors

Bi et al. reported a double-solvent approach to control the crystal growth, as well as a "controlled evaporative self-assembly" (CESA) method to realize the alignment of 2,5-di-(2-ethylhexyl)-3,6-bis(5″-n-hexyl-2,2′,5′,2″]terthiophen-5-yl)-pyrrolo[3,4-c] pyrrole-1,4-dione (SMDPPEH) [144]. The underlying mechanism involves the balance between nucleation density and crystal growth, where an optimal concentration facilitates uniform crystal formation and alignment. With SMDPPEH casted in chloroform, the organic semiconductor material formed a few microcrystals that randomly scattered over the substrate (Figure 2a). When chloroform and ethanol were employed as the double solvents (chloroform/ethanol at a ratio of 15:1, 10:1, 5:1, and 1:1), an enhanced density of crystals was formed, although the crystals still lacked alignment and long-range uniformity (Figure 2b). When the CESA method was applied to control the SMDPPEH crystallization, it created a capillary force that guided the oriented growth of the organic semiconductor. The resultant enhanced morphology is shown in Figure 2c–f. The optimization of double solvents and simultaneous application of the CESA method led to the excellent alignment of CESA organic crystals. In addition, the grain width was noted to depend on the double-solvent ratio. In particular, a 5:1 ratio of chloroform/ethanol double solvents led to an optimized amount of nucleation seeds and density, and simultaneously the CESA method was noted to most effectively orient the organic crystal orientations of SMDPPEH and contributed to an enhanced mobility of 0.016 cm^2/Vs. Therefore, a chloroform/ethanol ratio of 5:1 was found to be optimal for inducing nucleation and enhancing crystal density without compromising alignment. This ratio was crucial as it balanced the solvent evaporation rate, facilitating better control over crystal growth and alignment.

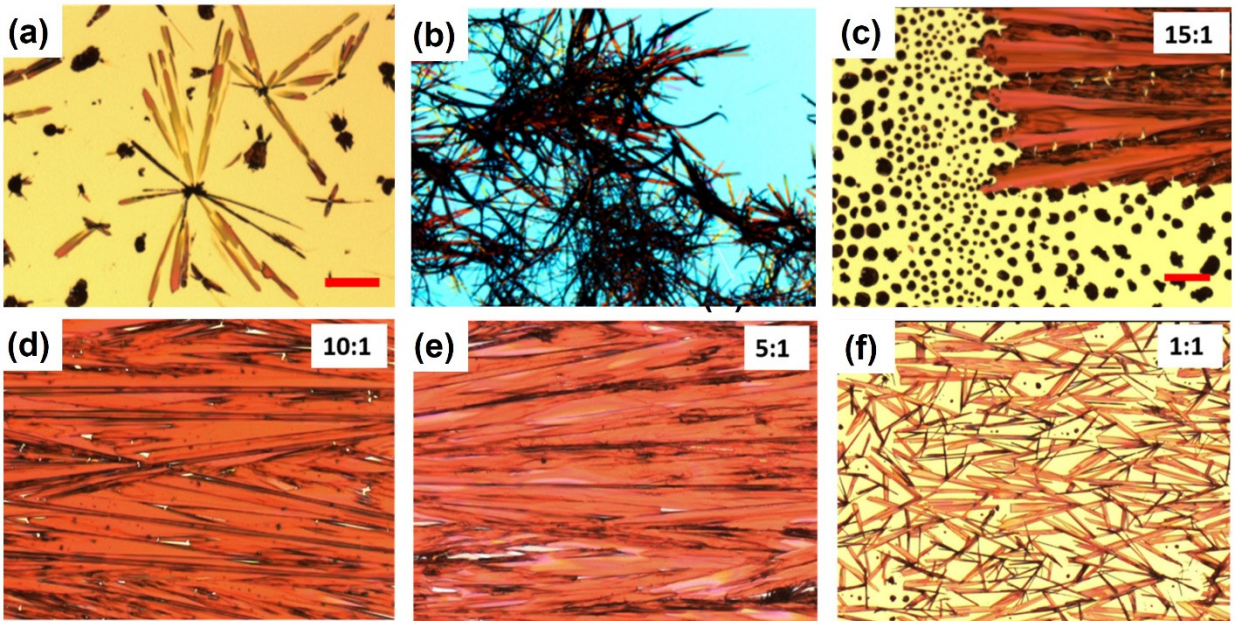

Figure 2. Optical images of SMDPPEH microcrystals obtained from drop-casting in various solvents, including (**a**) chloroform and chloroform/ethanol at the ratio of (**b**) 5:1, (**c**) 15:1, (**d**) 10:1, (**e**) 5:1, and (**f**) 1:1. CESA method was applied to orient and control the SMDPPEH crystals in (**c**–**f**). Images (**a**,**b**) have the same scale bar of 100 μm, as in (**a**), whereas images in (**c**–**f**) have the identical scale bar of 100 μm, as in (**c**). Reproduced from reference [144] with permission from American Institute of Physics.

Besides the application of the CESA alignment and binary solvent method, Bi et al. also reported the mixing of SMDPPEH with P3HT to modulate its crystallization and morphology [145]. SMDPPEH was mixed with P3HT in a single solvent of chloroform at a weight ratio of 5:1, and the mixed solution was drop-casted on the substrate at various concentrations. The resultant morphologies of the SMDPPEH crystals are shown in Figure 3a–c as a function of different concentrations. At 1 mg/mL, the SMDPPEH crystals showed dash points (Figure 3a), implying such low concentration is insufficient for the semiconductor to continuously crystallize. When the concentration increases to 2 mg/mL, the SMDPPEH semiconductor formed well-aligned crystals with enhanced connection in the long range, as shown in Figure 3b. As the concentration further increases to 5 mg/mL, the morphology quickly deteriorated and many grain boundaries with crystalline defects populated (Figure 3c). The dependence of the SMDPPEH morphology on the solution concentration, as observed from the polarized microscopic optical images, is further confirmed by using scanning electron microscopy (Figure 3d–f). A mobility of 0.001 cm^2/Vs was measured from the SMDPPEH/P3HT thin-film transistors based on the optimized concentration of 2 mg/mL.

Shin et al. reported a "template-guided solution-shearing (TGSS)" method to grow well-aligned π-extended donor–acceptor diketopyrrolopyrrole-based conjugated polymers, i.e., PTDPP-DTTE [79]. PTDPP-DTTE is composed of dithienyl-diketopyrrolopyrrole (TDPP) as the acceptor monomer and di(thienothienyl)ethylene (DTTE) as the donor monomer. The PTDPP-DTTE was deposited by using different methods, including the spin-coating, solution-shearing, and TGSS methods. As compared to the spin-coated film, the counterpart based on solution shearing showed alignment of polymer chains and elongated domains towards the shearing direction. In contrast, the crystals based on the TGSS method showed enhanced alignment of polymer chains, favorable for charge transport. GI-XRD results showed that the π-π stacking distance of the PTDPP-DTTE polymer was reduced to 3.47 Å when prepared by the TGSS method, as compared to 3.67 Å when deposited by spin-coating, indicating the micro-patterned mold results in larger strain

between the PTDPP-DTTE polymer chains. Top-contact, bottom-gate transistors yielded a hole mobility of 3.13 cm^2/Vs, 4.77 cm^2/Vs, and 7.43 cm^2/Vs, based on the deposition method of spin-coating, solution shearing, and the TGSS method, respectively. The TGSS method significantly enhances polymer alignment and charge transport by reducing the π-π stacking distance and improving molecular packing. This method is scalable for large-area organic electronics, as demonstrated by the uniformity of the films produced in our study. However, challenges such as maintaining uniform crystal orientation across larger substrates and controlling the shear rate and solvent evaporation uniformly must be addressed to ensure consistent performance across large areas.

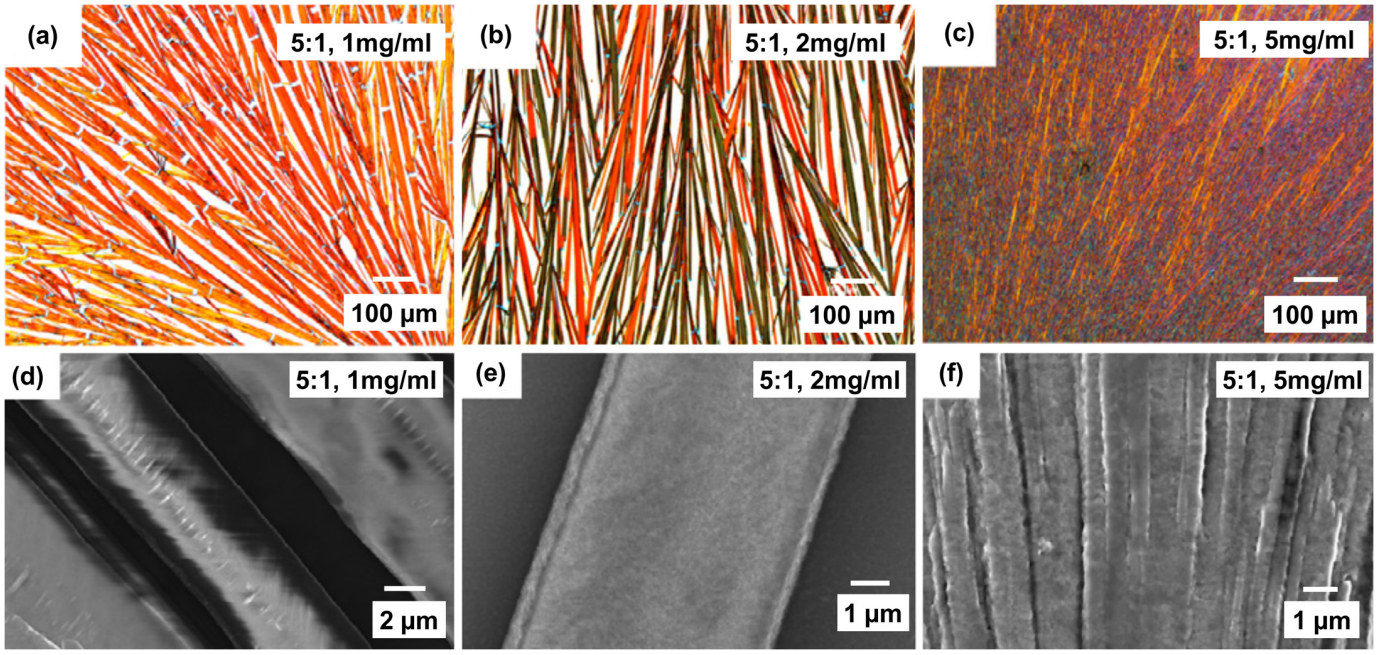

Figure 3. Optical images of SMDPPEH crystals with the P3HT additive at a 5:1 weight ratio based on different concentrations, including (**a**) 1, (**b**) 2, and (**c**) 5 mg/mL. The SEM images based on the same weight ratio and concentration as in (**a**–**c**) are shown in (**d**–**f**). Reproduced from reference [145] with permission from Elsevier.

The different studies reviewed in this section are summarized in Table 2.

Table 2. Summary of the different works reviewed in this section, including the diketopyrrolopyrrole-based semiconductors, *p*-type or *n*-type, the result findings, and mobility.

Author	Semiconductor	Type	Result Findings	Mobility
Bi et al. [144]	SMDPPEH	*p*-type	A "controlled evaporative self-assembly" method aligned crystal orientations	0.016 cm^2/Vs
Bi et al. [145]	SMDPPEH	*p*-type	P3HT was used as a polymer additive to modulate morphology and alignment	0.001 cm^2/Vs
Shin et al. [79]	PTDPP-DTTE	*p*-type	A "template-guided solution-shearing" method oriented crystals	7.43 cm^2/Vs based on the TGSS method

2.3. Thermal Annealing of Diketopyrrolopyrrole-Based Organic Semiconductors

The thermal properties of diketopyrrolopyrrole-based organic semiconductors differ significantly from those of inorganic semiconductors. Thermal annealing in these materials primarily enhances structural order and crystallinity, which are crucial for charge transport.

Chen et al. reported ambipolar copolymer DPPT-TT based on diketopyrrolopyrrole and thieno[3,2-b]thiophene for thin-film transistor applications [146]. Transistors were

fabricated based on a top-gate, bottom-contact configuration with poly(methyl methacrylate) (PMMA) as the gate dielectric layer. The effect of thermal annealing and the cleaning procedure of the gold electrodes was investigated on the charge transport of DPPT-TT semiconductors. Annealing at 320 °C reduces the electron-trapping impurities, decreases the contact resistance, and also improves the physical contact between the semiconductor and electrodes, which is favorable for charge transport. The optimal annealing temperature of 320 °C for DPPT-TT was determined based on its effect on reducing electron-trapping impurities, improving contact resistance, and enhancing physical contact between the semiconductor and electrodes. Thermal stability at this temperature ensures that the semiconductor maintains its performance by preserving the structural order and crystallinity. On the other hand, solvent cleaning of the gold electrodes prior to the deposition of DPPT-TT effectively modulates the gold work function to 4.7~4.9 eV, which facilitates electron injection. As a result, a1.36 ± 0.26 cm^2/Vs (hole mobility) and 1.56 ± 0.49 cm^2/Vs (electron mobility) were yielded from the DPPT-TT based on thermal annealing at 320 °C and the solvent cleaning of gold contact electrodes.

Nelson et al. studied film topography and charge transport of poly[2,5-dihexadecyl-3-5-[4-(2-hexyl-decyl)-4H-dithieno [3,2-b;2′, 3′-d] pyrrol-2-yl]-thiophen-2-yl-6-thiophen-2-yl-2,5-dihydropyrrolo[3,4-c]pyrrole-1,4-dione] (PDDTP-DPP) [147]. The molecular structure of DPPTP-DPP as a donor–acceptor polymer is shown in Figure 1. The low bandgap PDDTP-DPP is composed of a strong donor DTP and a strong acceptor DPP. Transistors were made by patterning the gold source and drain electrodes with photolithography. OTS treatment was performed on the substrate before drop-casting the PDDTP-DPP polymer to form the active layer. The PDDTP-DPP film after thermal annealing exhibited mobilities correlated with the conducting channel length. In particular, a maximum hole mobility of 0.41 cm^2/Vs was obtained based on 30 µm channel length. AFM imaging showed fine isotropic morphology composed of granular features rather than nanofibrillar morphology. Grazing incidence wide-angle X-ray scattering (GIWAXS) results indicated improved structural order after thermal annealing, responsible for the enhanced mobility.

Sonar et al. reported an ambipolar copolymer incorporating both a diketopyrrolopyrrole moiety and thiophene-benzothiadiazole-thiophene (TBT) as the donor–acceptor–donor building block [148]. The copolymer PDPP-TBT formed an active layer via spin coating, followed by thermal annealing. The AFM images of the PDPP-TBT films were presented in Figure 4a–d with different thermal annealing temperatures, including 120 °C, 180 °C, and 200 °C. While the PDPP-TBT film without annealing showed clustered nanofibers, these nanofibers increasingly prevail and form densely packed networks interconnecting the crystal domains as the thermal annealing temperature increases. Accordingly, the XRD spectra in Figure 4g showed enhanced peak intensities with increasing thermal annealing temperature. Thin-film transistors were fabricated by depositing the PDPP-TBT copolymers onto OTS-treated substrates and conducted with thermal annealing, yielding decent device performance in *p*- and *n*-channel modes, as shown in Figure 4e,f. The highest mobility values of 0.35 cm^2/Vs (hole) and 0.4 cm^2/Vs (electron) were obtained with thermal annealing at 200 °C.

Shahid et al. reported two selenophene-diketopyrrolopyrrole-based polymers, i.e., poly(3-(2,2′-biselenophen-5,5′-yl)-2,5-di(2-octyldodecyl)-6-(selenophen-2,5-yl)-1,4-diketopy rrolo[3,4-c]pyrrole (pDPPS3) and poly(3-(2,20-biselenophen-5,5′-yl)-2,5-di(2-octyldodecyl)-6-(thieno[3,2-b]thiophen-2,5-yl)-1,4-diketopyrrolo[3,4-c]pyrrole (pDPPS2TT), in an effort to lower the LUMO level in order to facilitate electron injection [149]. The synthesized pDPPS3 and pDPPS2TT polymers exhibit LUMO levels of 4 eV and 3.9 eV, respectively. After spin-coating the polymers onto HMDS-treated substrate, thermal annealing was found to play a vital role in enhancing the electrical charge transport, yielding a hole and electron mobility value of 0.1 cm^2/Vs for pDPPS3, as well as hole and electron mobility values of 0.3 cm^2/Vs and 0.05 cm^2/Vs for pDPPS2TT. In comparison, enhanced hole and electron mobility values of 1.1 cm^2/Vs and 0.15 cm^2/Vs were showcased from pDPPS3.

XRD results showed sharpened and intensified peak intensities for both polymers after thermal annealing, indicating enhanced crystallinity.

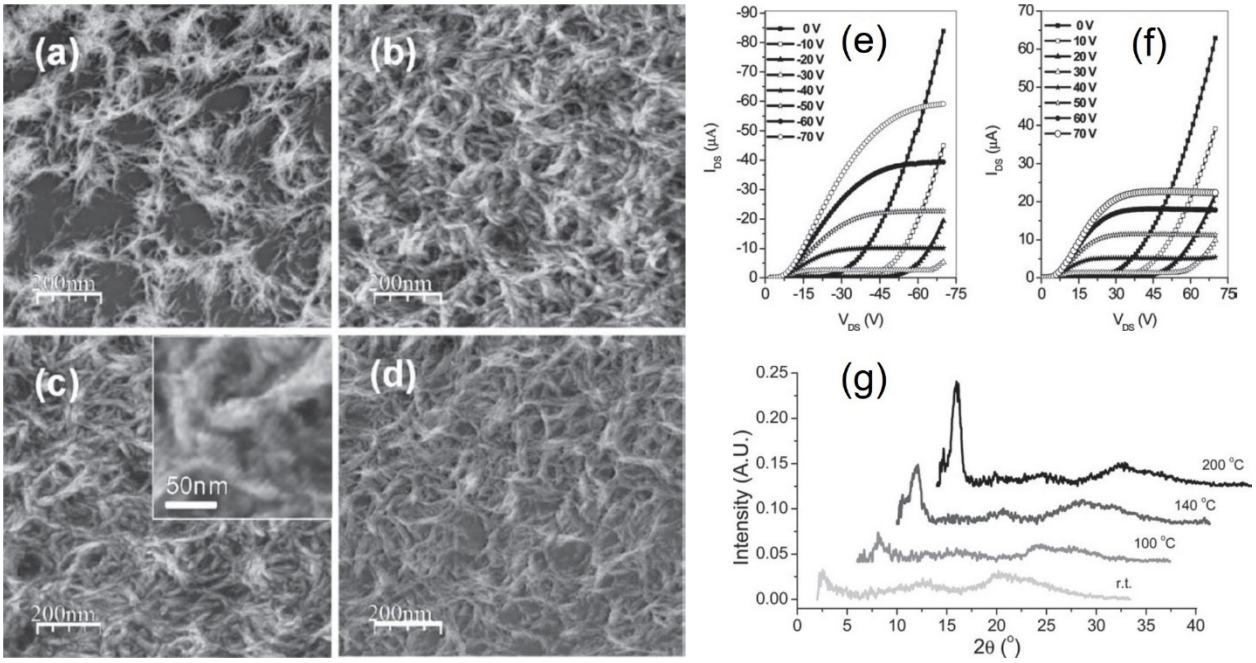

Figure 4. AFM images showing the PDPP-TBT after thermal annealing at (**a**) room temperature, (**b**) 120 °C, (**c**) 180 °C, and (**d**) 200 °C. (**e**,**f**) show the output characteristics for the *p*- and *n*-channel modes, respectively. The thermal annealing was conducted at 200 °C. (**g**) XRD spectra of the PDPP-TBT thin films with different annealing temperatures. Reproduced from reference [148] with permission from Wiley.

The different studies reviewed in this section are summarized in Table 3.

Table 3. Summary of the different works reviewed in this section, including the diketopyrrolopyrrole-based semiconductors, *p*-type or *n*-type, the result findings, and mobility.

Author	Semiconductor	Type	Result Findings	Mobility
Chen et al. [146]	DPPT-TT	Ambipolar	Thermal annealing and cleaning procedure of gold contacts impact the ambipolar behaviors of DPP-TT	1.36 ± 0.26 cm^2/Vs (hole) and 1.56 ± 0.49 cm^2/Vs (electron)
Nelson et al. [147]	PDDTP-DPP	*p*-type	Thermal annealing enhanced structural order and led to fine isotropic morphology	0.41 cm^2/Vs (hole)
Sonar et al. [148]	PDPP-TBT	Ambipolar	Thermal annealing modulated crystalline structure, charge transport	0.35 cm^2/Vs (hole) and 0.4 cm^2/Vs (electron)
Shahid et al. [149]	pDPPS3, pDPPS2TT	Ambipolar	Thermal annealing impacted crystallinity and charge transport of the polymers	1.1 cm^2/Vs (hole) and 0.15 cm^2/Vs (electron) from pDPPS3

2.4. Molecular Engineering of Diketopyrrolopyrrole-Based Organic Semiconductors

Tang et al. reported three conjugated small-molecular semiconductors based on diketopyrrolopyrrole, which comprise a diketopyrrolopyrrole core [107]. These three small molecules, i.e., 2TzDPPA1-2DCV, 2TzDPPA2-2DCV, and 2TzDPPA3-2DCV, have the same branching location at the nitrogen atoms, as shown in Figure 1, but the alkyl side-chain differs in its length. In particular, side chains of 2-hexyldecyl, 2-octyldodecyl and 2-decyltetradecyl were attached to 2TzDPPA1-2DCV, 2TzDPPA2-2DCV, and 2TzDPPA3-

2DCV, respectively. Side-chain length in 2TzDPPA derivatives plays a pivotal role in determining film morphology, molecular packing, and charge transport properties. Shorter side chains lead to more orderly packing and smoother film morphology, which enhances electron mobility. The key molecular design principles include optimizing side-chain length to balance crystallinity and film uniformity, thereby maximizing charge transport efficiency. AFM imaging results indicated that 2TzDPPA1-2DCV with a shorter side chain exhibited more uniform and continuous film topography. XRD implied that 2TzDPPA1-2DCV shows the largest *d*-spacing as a result of end-to-end packing, whereas 2TzDPPA3-2DCV shows the smallest *d*-spacing because of its interlaced packing between the alkyl side chain and the D diketopyrrolopyrrole PP core. After spin-coating the various diketopyrrolopyrrole-based small molecules onto octadecyltrimethoxysilane (OTS)-treated silicon dioxide to form an active layer, electrical characterization indicated an electron mobility of up to 0.28 cm^2/Vs, 0.13 cm^2/Vs, and 0.25 cm^2/Vs for 2TzDPPA1-2DCV, 2TzDPPA2-2DCV, and 2TzDPPA3-2DCV, respectively.

Shin et al. reported four π-extended conjugated polymers based on thienothiophene-flanked diketopyrrolopyrrole (DPPTT) with different side chains, including 2-octyldodecyl (PDPPTT-T-10), 2-decyltetradecyl (PDPPTT-T-12), 2-tetradecylhexadecyl (PDPPTT-T-14), 2-hexadecyloctadecyl (PDPPTT-T-16), and 2-octadecyldocosyl (PDPPTT-T-18) [150]. Depositing those conjugated polymers onto OTS-treated substrate yielded *p*-type transistor behaviors for all types of semiconductors. The highest mobility values of 1.23 cm^2/Vs, 0.16 cm^2/Vs, 1.92 cm^2/Vs, 0.35 cm^2/Vs, and 0.14 cm^2/Vs were obtained from PDPPTT-T-10, -12, -14, -16, and -18, respectively. The highest hole mobilities from PDPPTT-T-10 and -14 were attributed to the smooth surfaces with reduced roughness, as shown in Figure 5a–e. Additionally, the XRD spectra in Figure 5f,g show high crystallinity for PDPPTT-T-10 and -14, which adopt well-ordered lamellar structures with a dominant edge-on orientation (Figure 5h). In particular, the PDPPTT-T-14 film exhibited the smallest π–π stacking distance out of all five conjugated polymers, which is responsible for its highest mobility.

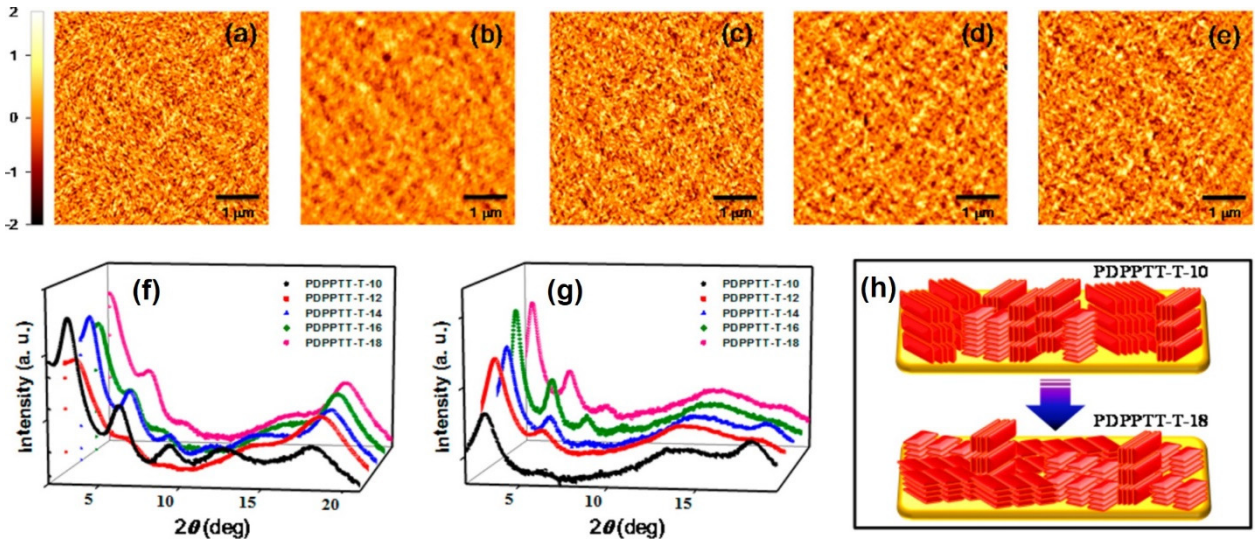

Figure 5. AFM height images the various conjugated polymers, including (**a**) PDPPTT-T-10, (**b**) -12, (**c**) -14, (**d**) -16, and (**e**) -18. (**f**) Out-of-plane and (**g**) in-plane XRD spectra of the conjugated polymers. (**h**) A schematic drawing showing the transition of molecular packing from PDPPTT-T-10 to -18 as respective to the substrates. Reproduced from reference [150] with permission from ACS Publications.

Chen et al. reported two donor–acceptor copolymers, poly[2,5-bis(alkyl)pyrrolo[3,4-c]pyrrole-1,4(2H, 5H)-dione-alt-5,5′-di(thiophen-2-yl)-2,2′-(E)-2-(2-(thiophen-2-yl)vinyl) thiophene] (PDVTs), which are attached with two alkyl side chains with different lengths [80]. In particular, PDVT-8 has a short side chain of a 2-octyldodecyl group, whereas PDVT-10 has a longer side chain of a 2-decyltetradecyl group. With thermal annealing at 180 °C,

the resultant thin-film topography is shown in Figure 6a–d. Both PDVT-8 and PDVT-10 films exhibit uniform intertwined fibers after spin-coating and enlarged polycrystalline grains with improved uniformity and interconnection after thermal annealing due to the intermolecular interactions between the copolymer backbones. Figure 6e,f show the grazing incidence out-of-plane and in-plane X-ray scattering of the PDVT-8 and PDVT-10 films after thermal annealing. Both films exhibit sharp (100) diffraction peaks with an edge-on packing structure. A π-π stacking distance of 3.72 Å and 3.66 Å was measured for PDVT-8 and PDVT-10. Transistors yielded a hole mobility of 4.5 cm^2/Vs and 8.2 cm^2/Vs for PDVT-8 and PDVT-10. The larger mobility of PDVT-10 is due to its enhanced topography uniformity and smaller π-π stacking distance. This study provides a detailed correlation between XRD data, AFM images, and transistor performance in PDVT-based copolymers. XRD analysis reveals the degree of crystallinity and π-π stacking distances, while AFM images illustrate the film morphology. These structural characteristics directly correlate with the measured transistor mobilities, highlighting the relationship between molecular packing, crystallinity, and device performance.

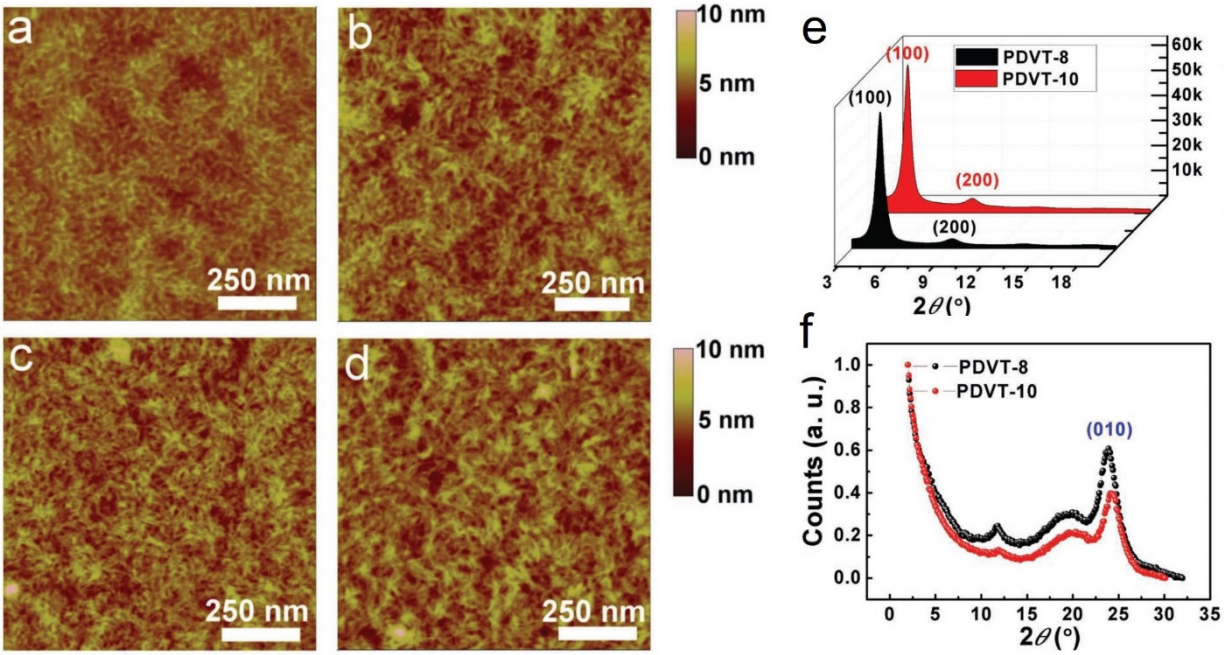

Figure 6. AFM topography images of (**a**,**b**) PDVT-8 and (**c**,**d**) PDVT-10 polymer films. (**a**,**c**) are based on no annealing, whereas (**b**,**d**) are based on annealing at 180 °C. (**e**) Grazing incidence out-of-plane X-ray scattering and (**f**) in-plane X-ray scattering based on annealing at 180 °C. Reproduced from reference [80] with permission from Wiley.

Yun et al. reported a copolymer poly[2,5-bis(2-octyldodecyl)pyrrolo[3,4-c] pyrrole-1,4(2H, 5H)-dione-(E)-[2,2′-bithiophen]-5-yl)-3-(thiophen-2-yl)acrylonitrile] (PDPP-CNTVT), which has an inclusion of a nitrile group in the polymer vinyl linkage, and compared its electrical performance with another diketopyrrolopyrrole-based copolymer (poly[2,5-bis(2-octyldodecyl) pyrrolo[3,4-c]pyrrole-1,4(2H,5H)-dione-(E)-1,2-di(2,2′-bithiophen-5-yl)ethene]) (PDPP-TVT) [81]. After spin-coating PDPP-CNTVT and PDPP-TVT onto prepatterned gold electrodes, depositing PMMA as gate dielectric layer and thermally evaporating Al as top-gate electrode, the transfer curves, as plotted in Figure 7a,b, show a dominant *p*-type behavior for PDPP-TVT and ambipolar behavior for PDPP-CNTVT. The device performance was further optimized by varying the solution concentration and modulating the active layer thickness. As shown in Figure 7c, reduction in the PDPP-CNTVT thickness results in a higher electron mobility of 7 cm^2/Vs. The enhanced charge transport in a thinner PDPP-CNTVT layer was attributed to the lower contact resistance and lesser presence of electron trapping sites in the bulk active layer, as illustrated in Figure 7d.

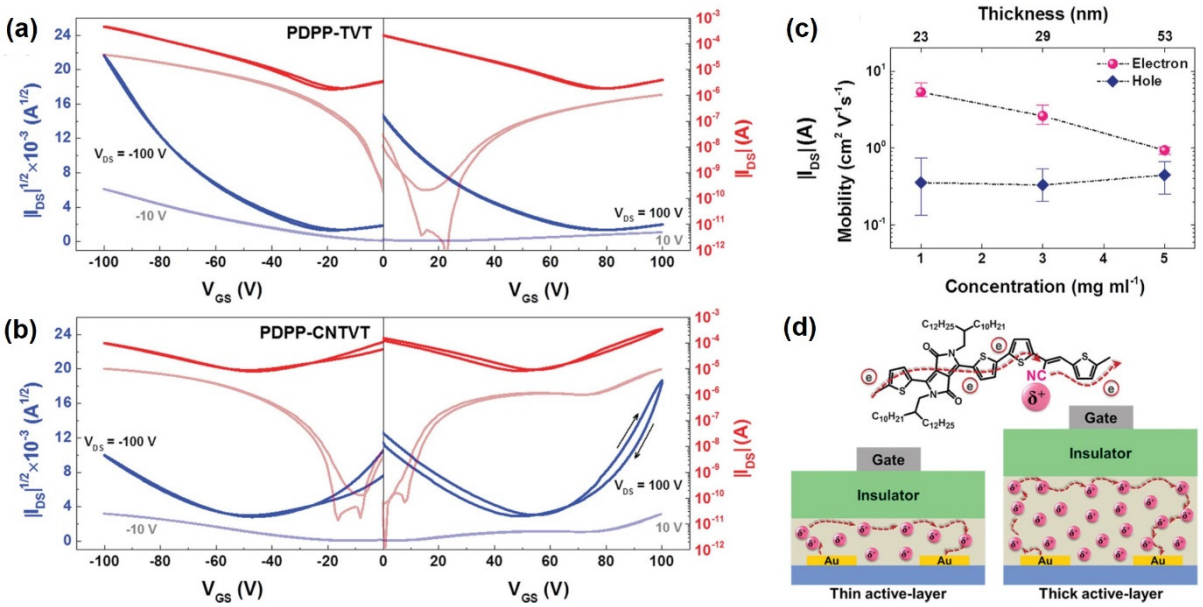

Figure 7. Ambipolar transfer curves of bottom-contact transistors based on (**a**) PDPP-TVT with annealing at 200 °C and (**b**) PDPP-CNTVT with annealing at 310 °C. The blue curves in (**a**,**b**) correspond to the square root of the drain current, while the red curves correspond to the drain current. The two arrows in the right figure of (**b**) indicate the presence of hysteresis in the transfer characteristics. (**c**) Correlation between the extracted charge-carrier mobilities, solution concentration, and active layer thickness of PDPP-CNTVT. (**d**) A schematic plot illustrating the transport and trapping of electron charge carriers in two different cases with different active layer thicknesses. Reproduced from reference [81] with permission from Wiley.

The different studies reviewed in this section are summarized in Table 4.

Table 4. Summary of the different works reviewed in this section, including the diketopyrrolopyrrole-based semiconductors, *p*-type or *n*-type, the result findings, and mobility.

Author	Semiconductor	Type	Result Findings	Mobility
Tang et al. [107]	2TzDPPA1-2DCV, 2TzDPPA2-2DCV, 2TzDPPA3-2DCV	*n*-type	Shorter alkyl side chain leads to more continuous topography and more orderly packing, favoring charge transport	0.28 cm^2/Vs from 2TzDPPA1-2DCV
Shin et al. [150]	PDPPTT-T-10, -12, -14, -16, -18	*p*-type	Attachment of 2-tetradecylhexadecyl side group leads to enhanced crystallinity, surface uniformity, and orderly packing	1.92 cm^2/Vs from PDPPTT-T-14
Chen et al. [80]	PDVT-8, PDVT-10	*p*-type	PDVT-10 with a longer side chain shows enhanced topography uniformity and smaller π-π stacking distance	8.2 cm^2/Vs from PDVT-10
Yun et al. [81]	PDPP-CNTVT	Ambipolar	Inclusion of a nitrile group in the polymer vinyl linkage results in ambipolar behavior; charge transport depends on active layer thickness	Electron mobility of 7 cm^2/Vs

2.5. Other Works on Diketopyrrolopyrrole-Based Organic Semiconductors

Kanimozhi et al. reported a conjugated copolymer, i.e., N-CS2DPP-OD-TEG, based on diketopyrrolopyrrole and diketopyrrolopyrrole (DPP-DPP) [151]. In this work, functionalized with triethylene glycol chains, the diketopyrrolopyrrole unit was then synthesized to form the high-molecular-weight copolymer DPP-DPP. For the bottom-gate transistors, a low balanced hole and electron mobility of ~0.01 cm^2/Vs was obtained. In contrast, a much higher electron mobility of 3 cm^2/Vs was demonstrated for the top-gate counterparts, which was attributed to the high-quality charge transport interface between the DPP-DPP organic semiconductor and the CYTOP gate dielectric layer.

Bronstein et al. prepared a polymer, namely P1, based on the copolymerization of both thieno[3,2-b]thiophene and diketopyrrolopyrrole [152]. Although ambipolar electrical performance of the devices was observed, a low electron mobility of 0.03 cm^2/Vs, as well as a much higher hole mobility of up to 1.95 cm^2/Vs, was reported from the thin-film transistors without employing thermal annealing at a high temperature. In addition, heterojunction solar cells incorporating the polymer and $PC_{71}BM$ exhibited an energy efficiency of 5.4%. This study shows that interface engineering is critical in optimizing the interaction between the semiconductor and dielectric layers, directly influencing device performance. For polymers such as P1 with low electron mobility, strategies such as modifying the dielectric interface, using interfacial layers, or adjusting the work function of electrodes can enhance electron mobility while maintaining or improving hole mobility.

Wang et al. reported an ambipolar copolymer poly(diketopyrrolopyrrole-terthiophene) (PDPPHD-T3) based on hexyldecyl-substituted diketopyrrolopyrrole and thiophene for application in xylene sensors [153]. In this work, a diketopyrrolopyrrole block was attached with a long alkyl chain to enhance the solution processability of the polymer. Transistors based on the PDPPHD-T3 copolymer and OTS-treated substrate showed a hole and electron mobility of 0.125 cm^2/Vs and 0.027 cm^2/Vs, respectively. Exposure to xylene vapors increased HOMO and LUMO levels of the PDPPHD-T3 polymer. Such energy level changes reduced the barrier for hole injection but increased that for electron injection, which modulated the electrical behaviors of the PDPPHD-T3-based thin-film transistor. As a result, the PDPPHD-T3 transistor-based sensor showed capability for detecting xylene at 40 ppm. This study shows PDPPHD-T3 polymer exhibits promising sensitivity and selectivity for xylene detection, with a response time that compares favorably to existing sensors. These results indicate that the sensor can detect xylene concentrations as low as 40 ppm, with rapid response and recovery times. The sensitivity is attributed to the modulation of energy levels upon xylene exposure, which influences the charge transport properties.

Li et al. reported a donor–acceptor polymeric organic semiconductor PDQT which comprises diketopyrrolopyrrole and β-unsubstituted quaterthiophene (QT) [78]. Without applying thermal annealing, PDQT forms layer-by-layer lamellar crystalline structures. The strong intermolecular interactions between the diketopyrrolopyrrole moieties, as well as the those between the DPP-QT donor–acceptor, induce the polymer chains to spontaneously form self-assembled structures of close proximity with a large π–π overlap. These interconnected crystalline structures provide an efficient intergranular charge transport pathway. The effect from thermal annealing and molecular weight on the thin-film topography was studied by using AFM (Figure 8a–f). The PDQT polymer morphology was observed to depend on its molecular weight. For PDQT with a high molecular weight, densely packed grains were formed with nanometer size, whereas for the counterpart with a low molecular weight, the film was found to be present with pinholes that deteriorate the interconnected structure. Transistors were fabricated by depositing the PDQT polymer onto OTS-treated substrates, which yielded *p*-type electrical behaviors, as shown in the output and transfer curves in Figure 8g–j. A mobility of 0.89 cm^2/Vs was obtained from the high-molecular-weight PDQT-based thin-film transistors, which further increased to 0.97 cm^2/Vs when the crystalline film was thermally annealed at 100 °C. In contrast, the low-molecular-weight PDQT-based devices fabricated using the same conditions exhibited only a lower mobility of 0.35–0.39 cm^2/Vs.

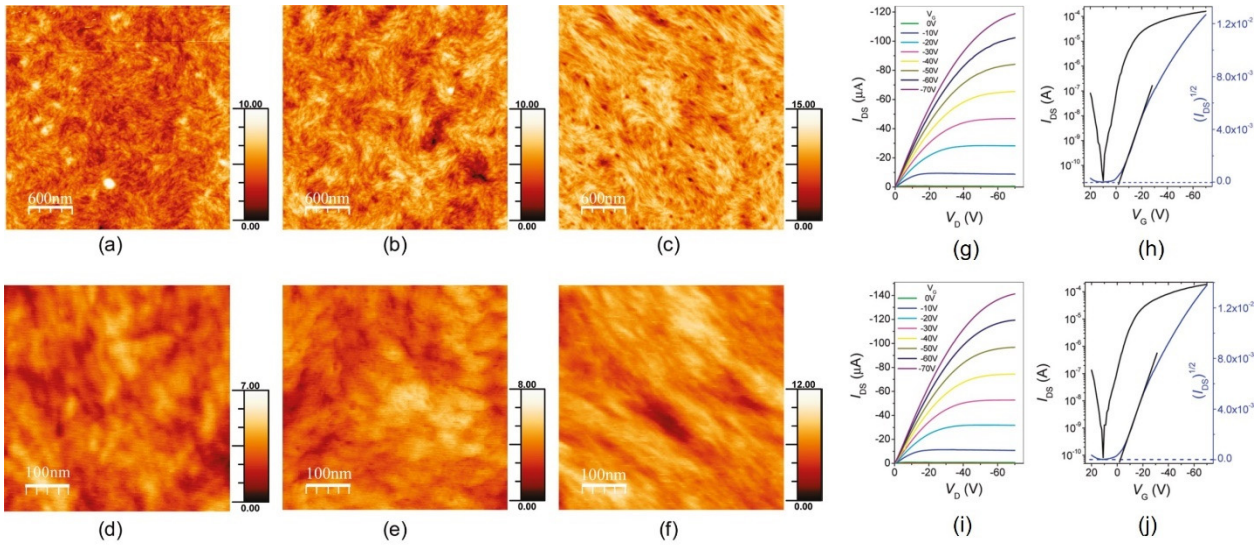

Figure 8. AFM height images showing (**a**,**d**) high-molecular-weight PDQT film, (**b**,**e**) high-molecular-weight PDQT film annealed at100 °C, and (**c**,**f**) low-molecular-weight PDQT thin film annealed at 100 °C. Output and transfer characteristics of high-molecular-weight PDQT-based thin-film transistors (**g**,**h**) without thermal annealing and (**i**,**j**) annealed at 100 °C. Reproduced from reference [78] with permission from ACS Publications.

The different studies reviewed in this section are summarized in Table 5.

Table 5. Summary of the different works reviewed in this section, including the diketopyrrolopyrrole-based semiconductors, *p*-type or *n*-type, the result findings, and mobility.

Author	Semiconductor	Type	Result Findings	Mobility
Kanimozhi et al. [151]	N-CS2DPP-OD-TEG	Ambipolar	Device configuration impacts ambipolar behaviors and charge transport	3 cm^2/Vs (electron)
Bronstein et al. [152]	Diketopyrrolopyrrole based polymer	Ambipolar	A much higher hole mobility was obtained than electron mobility	1.95 cm^2/Vs (hole)
Wang et al. [153]	PDPPHD-T3	Ambipolar	Device performance of PDPPHD-T3 thin-film transistor for detecting xylene	0.125 cm^2/Vs (hole) and 0.027 cm^2/Vs (electron)
Li et al. [78]	PDQT	*p*-type	High-molecular-weight PDQT exhibits more superior morphology and charge transport	0.97 cm^2/Vs from the high-molecular-weight PDQT

3. Conclusions and Outlook

In this article, we have reported a comprehensive review of the various efforts dedicated to achieving uniform crystal orientation, improving film morphology, and optimizing the charge carrier transport of small-molecular and polymeric organic semiconductors based on diketopyrrolopyrrole. First of all, external alignment contributes to aligned crystal orientations, controlled crystal growth, and improved charge carrier transport. Additionally, thermal annealing plays a vital role in modulating the ambipolar behaviors, enhanced structural order, film morphology, and semiconductor crystallinity. Furthermore, side-chain engineering results in enhanced π–π stacking distance, more orderly packing, improved crystallinity, enhanced topography, greater surface uniformity, and elevated mobility. By discussing the category of external crystal alignment, thermal annealing, and molecular engineering of diketopyrrolopyrrole-based organic semiconductors, this work

demonstrates that these universal methods can be applied to other solution-processed organic semiconductors to improve their molecular packing, enhance film morphology and crystallinity, and boost charge transport properties.

Future works in the following fields will yield more exciting outcomes in the research of organic semiconductors and organic electronic devices. First, since small-molecular and polymeric organic semiconductors based on diketopyrrolopyrrole exhibit ambipolar behaviors, these attributes can find extensive applications in complimentary inverters and thereby open up exciting pathways for high-performance organic electronics. Second, in addition to the polymeric additives such as P3HT, other additives, including small-molecular additives [154–158] and nanostructured additives [159–164], have been documented to manipulate the nucleation seed deposition, crystal formation, and film morphology of other organic semiconductors such as TIPS pentacene. Mixing these small-molecular and nanostructured additives with diketopyrrolopyrrole-based organic semiconductors, therefore, will enable the tuning of nucleation, crystallization, and charge transport. Furthermore, it is well known that external force [165–170] contributes to rigid alignment of the organic crystals, whereas polymeric additives result in overall morphological uniformity. Therefore, it can be beneficial to combine external force alignment methods with polymeric additives [171–178] to control the crystallization and charge transport of diketopyrrolopyrrole-based semiconductors. We believe future endeavors in these aforementioned fields will unveil a promising roadmap to realizing high-performance organic electronics applications.

Funding: This research received no external funding.

Institutional Review Board Statement: Not applicable.

Informed Consent Statement: Not applicable.

Data Availability Statement: No new data were created or analyzed in this study.

Conflicts of Interest: The authors declare no conflict of interest.

References

1. Hu, P.; He, X.; Jiang, H. Greater than 10 cm^2 V^{-1} s^{-1}: A breakthrough of organic semiconductors for field-effect transistors. *InfoMat* **2021**, *3*, 613. [CrossRef]
2. Guo, J.; Yu, B.; Zhu, F.; Yan, D. Significant improvement of 2,9-DPh-DNTT organic thin-film transistors based on organic heterojunction buffer layer. *Org. Electron.* **2021**, *93*, 106159. [CrossRef]
3. Xie, P.; Liu, T.; Sun, J.; Jiang, J.; Yuan, Y.; Gao, Y.; Zhou, J.; Yang, J. Solution-processed ultra-flexible C8-BTBT organic thin-film transistors with the corrected mobility over 18 cm^2/(V s). *Sci. Bull.* **2020**, *65*, 791. [CrossRef]
4. Sánchez Vergara, M.E.; Santillán Esquivel, E.A.; Ballinas-Indilí, R.; Lozada-Flores, O.; Miranda-Ruvalcaba, R.; Álvarez-Toledano, C. Organic Semiconductor Devices Fabricated with Recycled Tetra Pak®-Based Electrodes and *para*-Quinone Methides. *Coatings* **2024**, *14*, 998. [CrossRef]
5. Morab, S.; Sundaram, M.M.; Pivrikas, A. Review on Charge Carrier Transport in Inorganic and Organic Semiconductors. *Coatings* **2023**, *13*, 1657. [CrossRef]
6. Orgiu, E.; Samori, P. 25th Anniversary Article: Organic Electronics Marries Photochromism: Generation of Multifunctional Interfaces, Materials, and Devices. *Adv. Mater.* **2014**, *26*, 1827. [CrossRef] [PubMed]
7. Park, S.; Lee, B.; Bae, B.; Chai, J.; Lee, S.; Kim, C. Ambipolar thin-film transistors based on organic semiconductor blend. *Synth. Met.* **2019**, *253*, 40. [CrossRef]
8. Lee, J.; Kwon, J.; Lim, J.; Lee, C. An Amorphous Polythiophene as a Binder Material for Organic Thin-Film Transistor Channel Applications. *Mol. Cryst. Liq. Cryst.* **2010**, *519*, 179. [CrossRef]
9. Tazuhara, S.; Nagase, T.; Kobayashi, T.; Sadamitsu, Y.; Naito, H. Understanding the influence of contact resistances on short-channel high-mobility organic transistors in linear and saturation regimes. *Appl. Phys. Express* **2021**, *14*, 041010. [CrossRef]
10. Tripathi, A.K.; Heinrich, M.; Siegrist, T.; Pflaum, J. Growth and Electronic Transport in 9,10-Diphenylanthracene Single Crystals—An Organic Semiconductor of High Electron and Hole Mobility. *Adv. Mater.* **2007**, *19*, 2097. [CrossRef]
11. Xue, G.; Wu, J.; Fan, C.; Liu, S.; Huang, Z.; Liu, Y.; Shan, B.; Xin, H.L.; Miao, Q.; Chen, H.; et al. Boosting the electron mobility of solution-grown organic single crystals via reducing the amount of polar solvent residues. *Mater. Horiz.* **2016**, *3*, 119. [CrossRef]
12. Liu, J.; Zhang, H.; Dong, H.; Meng, L.; Jiang, L.; Jiang, L.; Wang, Y.; Yu, J.; Sun, Y.; Hu, W.; et al. High mobility emissive organic semiconductor. *Nat. Commun.* **2015**, *6*, 10032. [CrossRef] [PubMed]
13. Jurchescu, O.D.; Popinciuc, M.; van Wees, B.J.; Palstra, T.T.M. Interface-Controlled, High-Mobility Organic Transistors. *Adv. Mater.* **2007**, *19*, 688. [CrossRef]

14. Lee, B.H.; Kim, S.; Lee, S.Y. Ammonia Gas Sensing Properties of 6,13-Bis(tri-isopropylsilyethynyl) Pentacene Based Field-Effect Transistor. *Trans. Electr. Electron. Mater.* **2022**, *23*, 182–186. [CrossRef]
15. Hou, S.; Zhuang, X.; Fan, H.; Yu, J. Grain Boundary Control of Organic Semiconductors via Solvent Vapor Annealing for High-Sensitivity NO_2 Detection. *Sensors* **2021**, *21*, 226. [CrossRef]
16. Benavides, C.M.; Biele, M.; Schmidt, O.; Brabec, C.J.; Tedde, S.F. TIPS Pentacene as a Beneficial Interlayer for Organic Photodetectors in Imaging Applications. *IEEE Trans. Electron Devices* **2018**, *65*, 1516. [CrossRef]
17. Zhao, X.; Liu, T.; Liu, H.; Wang, S.; Li, X.; Zhang, Y.; Hou, X.; Liu, Z.; Shi, W.; Dennis, T.J.S. Organic Single-Crystalline p–n Heterojunctions for High-Performance Ambipolar Field-Effect Transistors and Broadband Photodetectors. *ACS Appl. Mater. Interfaces* **2018**, *10*, 42715. [CrossRef]
18. Jea, M.; Kumar, A.; Cho, H.; Yang, D.; Shim, H.; Palai, A.K.; Pyo, S. An organic microcrystal array-embedded layer: Highly directional alternating p- and n-channels for ambipolar transistors and inverters. *J. Mater. Chem. C* **2014**, *2*, 3980. [CrossRef]
19. Janneck, R.; Nowack, T.S.; De Roose, F.; Ali, H.; Dehaene, W.; Heremans, P.; Genoe, J.; Rolin, C. Integration of highly crystalline C8-BTBT thin-films into simple logic gates and circuits. *Org. Electron.* **2019**, *67*, 64. [CrossRef]
20. Chen, Z.; Duan, S.; Zhang, X.; Hu, W. Novel solution-processed 2D organic semiconductor crystals for high-performance OFETs. *Mater. Chem. Front.* **2024**, *8*, 2227. [CrossRef]
21. Basu, R. A review on single crystal and thin film Si–Ge alloy: Growth and applications. *Mater. Adv.* **2022**, *3*, 4489. [CrossRef]
22. Sun, L.; Li, T.; Zhou, J.; Li, W.; Wu, Z.; Niu, R.; Cheng, J.; Asare-Yeboah, K.; He, Z. A Green Binary Solvent Method to Control Organic Semiconductor Crystallization. *ChemistrySelect* **2023**, *8*, e202203927. [CrossRef]
23. Bi, S.; Gao, B.; Han, X.; He, Z.; Metts, J.; Jiang, C.; Asare-Yeboah, K. Recent progress in printing flexible electronics: A review. *Sci. China Technol. Sci.* **2023**, *67*, 2363–2386. [CrossRef]
24. Wang, Y.; Han, X.; Jin, L.; Meng, Y.; Jiang, C.; Asare-Yeboah, K.; He, Z.; Bi, S. Excitation Threshold Reduction Techniques for Organic Semiconductor Lasers: A Review. *Coatings* **2023**, *13*, 1815. [CrossRef]
25. He, Z.; Zhang, Z.; Bi, S. Small-molecule additives for organic thin film transistors. *J. Mater. Sci. Mater. Electron.* **2019**, *30*, 20899. [CrossRef]
26. He, Z.; Zhang, Z.; Asare-Yeboah, K.; Bi, S. Poly(α-methylstyrene) polymer and small-molecule semiconductor blend with reduced crystal misorientation for organic thin film transistors. *J. Mater. Sci. Mater. Electron.* **2019**, *30*, 14335. [CrossRef]
27. Cho, S.; Lim, E. Controlling fabrication temperature of TIPS-pentacene to improve carrier properties. *J. Korean Phys. Soc.* **2023**, *82*, 91. [CrossRef]
28. He, Z.; Zhang, Z.; Bi, S. Long-range crystal alignment with polymer additive for organic thin film transistors. *J. Polym. Res.* **2019**, *26*, 173. [CrossRef]
29. Zhang, S.; Talnack, F.; Jousselin-Oba, T.; Bhat, V.; Wu, Y.; Lei, Y.; Tomo, Y.; Gong, H.; Michalek, L.; Zhong, D.; et al. Shear-aligned large-area organic semiconductor crystals through extended π–π interaction. *J. Mater. Chem. C* **2023**, *11*, 8992. [CrossRef]
30. He, Z.; Chen, J.; Li, D. Crystal alignment for high performance organic electronics devices. *J. Vac. Sci. Technol. A* **2019**, *37*, 040801. [CrossRef]
31. Tamayo, A.; Hofer, S.; Salzillo, T.; Ruzié, C.; Schweicher, G.; Resel, R.; Mas-Torrent, M. Mobility anisotropy in the herringbone structure of asymmetric Ph-BTBT-10 in solution sheared thin film transistors. *J. Mater. Chem. C* **2021**, *9*, 7186. [CrossRef]
32. He, Z.; Zhang, Z.; Bi, S.; Asare-Yeboah, K.; Chen, J. Ultra-low misorientation angle in small-molecule semiconductor/polyethylene oxide blends for organic thin film transistors. *J. Polym. Res.* **2020**, *27*, 75. [CrossRef]
33. Bai, J.; Jiang, Y.; Wang, Z.; Sui, Y.; Deng, Y.; Han, Y.; Geng, Y. Bar-Coated Organic Thin-Film Transistors with Reliable Electron Mobility Approaching 10 $cm^2\ V^{-1}\ s^{-1}$. *Adv. Electron. Mater.* **2020**, *6*, 1901002. [CrossRef]
34. He, Z.; Zhang, Z.; Bi, S. Polyacrylate Polymer Assisted Crystallization: Improved Charge Transport and Performance Consistency for Solution-Processable Small-Molecule Semiconductor Based Organic Thin Film Transistors. *J. Sci. Adv. Mater. Devices* **2019**, *4*, 467. [CrossRef]
35. Kim, N.-K.; Jang, S.-Y.; Pace, G.; Caironi, M.; Park, W.-T.; Khim, D.; Kim, J.; Kim, D.-Y.; Noh, Y.-Y. High-Performance Organic Field-Effect Transistors with Directionally Aligned Conjugated Polymer Film Deposited from Pre-Aggregated Solution. *Chem. Mater.* **2015**, *27*, 8345. [CrossRef]
36. Diao, Y.; Shaw, L.; Bao, Z.A.; Mannsfeld, S.C.B. Morphology control strategies for solution-processed organic semiconductor thin films. *Energy Environ. Sci.* **2014**, *7*, 2145. [CrossRef]
37. He, Z.; Bi, S.; Asare-Yeboah, K.; Zhang, Z. Phase segregation effect on TIPS pentacene crystallization and morphology for organic thin film transistors. *J. Mater. Sci. Mater. Electron.* **2020**, *31*, 4503. [CrossRef]
38. Chen, J.H.; Martin, D.C.; Anthony, J.E. Morphology and molecular orientation of thin-film bis(triisopropylsilylethynyl) pentacene. *J. Mater. Res.* **2007**, *22*, 1701. [CrossRef]
39. He, Z.; Lopez, N.; Chi, X.; Li, D. Solution-based 5,6,11,12-tetrachlorotetracene crystal growth for high-performance organic thin film transistors. *Org. Electron.* **2015**, *22*, 191. [CrossRef]
40. Chen, J.H.; Anthony, J.E.; Martin, D.C. Crystallographic cracking during a thermally-induced solid-state phase transition in TIPS pentacene. *Abstr. Pap. Am. Chem. Soc.* **2005**, *230*, 309.
41. He, Z.; Zhang, Z.; Bi, S.; Chen, J. Tuning charge transport in organic semiconductors with nanoparticles and hexamethyldisilazane. *J. Nanopart. Res.* **2021**, *23*, 5. [CrossRef]

42. Chi, X.L.; Li, D.W.; Zhang, H.Q.; Chen, Y.S.; Garcia, V.; Garcia, C.; Siegrist, T. 5,6,11,12-Tetrachlorotetracene, a tetracene derivative with pi-stacking structure: The synthesis, crystal structure and transistor properties. *Org. Electron.* **2008**, *9*, 234. [CrossRef]
43. Yagodkin, E.; Xia, Y.; Kalihari, V.; Frisbie, C.D.; Douglas, C.J. Synthesis, Solid State Properties, and Semiconductor Measurements of 5,6,11,12-Tetrachlorotetracene. *J. Phys. Chem. C* **2009**, *113*, 16544. [CrossRef]
44. Hwang, D.K.; Fuentes-Hernandez, C.; Kim, J.B.; Potscavage, W.J.; Kippelen, B. Flexible and stable solution-processed organic field-effect transistors. *Org. Electron.* **2011**, *12*, 1108. [CrossRef]
45. James, D.T.; Kjellander, B.K.C.; Smaal, W.T.T.; Gelinck, G.H.; Combe, C.; McCulloch, I.; Wilson, R.; Burroughes, J.H.; Bradley, D.D.C.; Kim, J.S. Thin-Film Morphology of Inkjet-Printed Single-Droplet Organic Transistors Using Polarized Raman Spectroscopy: Effect of Blending TIPS-Pentacene with Insulating Polymer. *Acs Nano* **2011**, *5*, 9824. [CrossRef]
46. Rogowski, R.Z.; Dzwilewski, A.; Kemerink, M.; Darhuber, A.A. Solution Processing of Semiconducting Organic Molecules for Tailored Charge Transport Properties. *J. Phys. Chem. C* **2011**, *115*, 11758. [CrossRef]
47. Li, Y.; Liu, C.; Kumatani, A.; Darmawan, P.; Minari, T.; Tsukagoshi, K. Patterning solution-processed organic single-crystal transistors with high device performance. *AIP Adv.* **2011**, *1*, 022149. [CrossRef]
48. Chen, J.H.; Tee, C.K.; Shtein, M.; Martin, D.C.; Anthony, J. Controlled solution deposition and systematic study of charge-transport anisotropy in single crystal and single-crystal textured TIPS pentacene thin films. *Org. Electron.* **2009**, *10*, 696. [CrossRef]
49. He, Z.; Asare-Yeboah, K.; Zhang, Z.; Bi, S. Manipulate organic crystal morphology and charge transport. *Org. Electron.* **2022**, *103*, 106448. [CrossRef]
50. Briseno, A.L.; Mannsfeld, S.C.B.; Ling, M.M.; Liu, S.H.; Tseng, R.J.; Reese, C.; Roberts, M.E.; Yang, Y.; Wudl, F.; Bao, Z.N. Patterning organic single-crystal transistor arrays. *Nature* **2006**, *444*, 913. [CrossRef]
51. Kuribara, K.; Nobeshima, T.; Takei, A.; Kodzasa, T.; Uemura, S.; Yoshida, M. Wettability control with self-assembler patterning for printed electronics. *Jpn. J. Appl. Phys.* **2019**, *58*, 041002. [CrossRef]
52. Chen, Z.; Duan, S.; Zhang, X.; Geng, B.; Xiao, Y.; Jie, J.; Dong, H.; Li, L.; Hu, W. Organic Semiconductor Crystal Engineering for High-Resolution Layer-Controlled 2D Crystal Arrays. *Adv. Mater.* **2021**, *34*, 2104166. [CrossRef]
53. Li, W.; Li, L.; Sun, Q.; Liu, X.; Kanehara, M.; Nakayama, T.; Jiu, J.; Sakamoto, K.; Minari, T. Direct fabrication of high-resolution and high-performance flexible electronics via surface-activation-localized electroless plating. *Chem. Eng. J.* **2021**, *416*, 127644. [CrossRef]
54. Kolodziejczyk, B.; Winther-Jensen, O.; Pereira, B.A.; Nair, S.S.; Winther-Jensen, B. Patterning of conducting layers on breathable substrates using laser engraving for gas sensors. *J. Appl. Polym. Sci.* **2015**, *132*, 42359. [CrossRef]
55. Jo, P.S.; Duong, D.T.; Park, J.; Sinclair, R.; Salleo, A. Control of Rubrene Polymorphs via Polymer Binders: Applications in Organic Field-Effect Transistors. *Chem. Mater.* **2015**, *27*, 3979. [CrossRef]
56. Wang, B.; Zhu, T.; Huang, L.; Tam, T.L.D.; Cui, Z.; Ding, J.; Chi, L. Addressable growth of oriented organic semiconductor ultra-thin films on hydrophobic surface by direct dip-coating. *Org. Electron.* **2015**, *24*, 170. [CrossRef]
57. Meng, Q.; Zhang, F.; Zang, Y.; Huang, D.; Zou, Y.; Liu, J.; Zhao, G.; Wang, Z.; Ji, D.; Di, C.-A.; et al. Solution-sheared ultrathin films for highly-sensitive ammonia detection using organic thin-film transistors. *J. Mater. Chem. C* **2014**, *2*, 1264. [CrossRef]
58. Kim, K.; Nam, K.; Li, X.; Lee, D.Y.; Kim, S.H. Programmed Design of Highly Crystalline Organic Semiconductor Patterns with Uniaxial Alignment via Blade Coating for High-Performance Organic Field-Effect. *ACS Appl. Mater. Interfaces* **2019**, *11*, 42403. [CrossRef] [PubMed]
59. Leonardi, F.; Zhang, Q.; Kim, Y.-H.; Mas-Torrent, M. Solution-sheared thin films of a donor-acceptor random copolymer-polystyrene blend as active material in field-effect transistors. *Mater. Sci. Semicond. Process.* **2019**, *93*, 105. [CrossRef]
60. Kwon, H.-J.; Kim, K.; An, T.K.; Kim, S.H.; Park, C.E. Effect of lateral confinement on crystallization behavior of a small-molecule semiconductor during capillary force lithography for use in high-performance OFETs. *J. Ind. Eng. Chem.* **2019**, *75*, 187. [CrossRef]
61. Park, Y.; Park, J.; Cho, S.; Sung, M.M. Large-area single-crystal organic patterned thin films by vertically confined lateral crystal growth via capillary force lithography. *Appl. Surf. Sci.* **2019**, *494*, 1023. [CrossRef]
62. Ma, X.; Liu, Q.; Xu, D.; Zhu, Y.; Kim, S.; Cui, Y.; Zhong, L.; Liu, M. Capillary-Force-Assisted Clean-Stamp Transfer of Two-Dimensional Materials. *Nano Lett.* **2017**, *17*, 6961. [CrossRef] [PubMed]
63. Schweicher, G.; Liu, G.; Fastré, P.; Resel, R.; Abbas, M.; Wantz, G.; Geerts, Y.H. Directional crystallization of C8-BTBT-C8 thin films in a temperature gradient. *Mater. Chem. Front.* **2021**, *5*, 249. [CrossRef]
64. Kneppe, D.; Talnack, F.; Boroujeni, B.K.; Teixeira da Rocha, C.; Höppner, M.; Tahn, A.; Mannsfeld, S.C.B.; Ellinger, F.; Leo, K.; Kleemann, H. Solution-processed pseudo-vertical organic transistors based on TIPS-pentacene. *Mater. Today Energy* **2021**, *21*, 100697. [CrossRef]
65. Yang, Z.; Lin, S.; Liu, J.; Zheng, K.; Lu, G.; Ye, B.; Huang, J.; Zhang, Y.; Ye, Y.; Guo, T.; et al. High performance phototransistors with organic/quantum dot composite materials channels. *Org. Electron.* **2020**, *78*, 105565. [CrossRef]
66. Najafi-Ashtiani, F. Low temperature processing of $BaTiO_3$-PMMA-PVP hybrid films as transparent dielectric gate. *J. Mater. Sci.-Mater. Electron.* **2019**, *30*, 7087. [CrossRef]
67. Haq, Y.-U.; Ullah, R.; Mazhar, S.; Khattak, R.; Qarni, A.A.; Haq, Z.-U.; Amin, S. Synthesis and characterization of 2D MXene: Device fabrication for humidity sensing. *J. Sci. Adv. Mater. Devices* **2021**, *7*, 100390. [CrossRef]
68. Powell, D.; Campbell, E.V.; Flannery, L.; Ogle, J.; Soss, S.E.; Whittaker-Brooks, L. Steric hindrance dependence on the spin and morphology properties of highly oriented self-doped organic small molecule thin films. *Mater. Adv.* **2021**, *2*, 356. [CrossRef]

69. Mohammed, H.Y.; Farea, M.A.; Sayyad, P.W.; Ingle, N.N.; Al-Gahouari, T.; Mahadik, M.M.; Bodkhe, G.A.; Shirsat, S.M.; Shirsat, M.D. Selective and sensitive chemiresistive sensors based on polyaniline/graphene oxide nanocomposite: A cost-effective approach. *J. Sci. Adv. Mater. Devices* **2021**, *7*, 100391. [CrossRef]
70. Yang, Z.; Lin, S.; Liu, J.; Zheng, K.; Lu, G.; Ye, B.; Huang, J.; Zhang, Y.; Ye, Y.; Guo, T.; et al. Sharp phase-separated interface of 6, 13-bis (triisopropylsilylethynyl) pentacene/polystyrene blend films prepared by electrostatic spray deposition. *Org. Electron.* **2020**, *78*, 206.
71. Park, M.; Cho, W.; Lee, G.; Hong, S.C.; Kim, M.C.; Yoon, J.; Ahn, N.; Choi, M. Highly Reproducible Large-Area Perovskite Solar Cell Fabrication via Continuous Megasonic Spray Coating of $CH_3NH_3PbI_3$. *Small* **2019**, *15*, 1804005. [CrossRef]
72. Koutsiaki, C.; Kaimakamis, T.; Zachariadis, A.; Papamichail, A.; Kamaraki, C.; Fachouri, S.; Gravalidis, C.; Laskarakis, A.; Logothetidis, S. Efficient combination of Roll-to-Roll compatible techniques towards the large area deposition of a polymer dielectric film and the solution-processing of an organic semiconductor for the field-effect transistors fabrication on plastic substrate. *Org. Electron.* **2019**, *73*, 231. [CrossRef]
73. Teisala, H.; Tuominen, M.; Stepien, M.; Haapanen, J.; Makela, J.M.; Saarinen, J.J.; Toivakka, M.; Kuusipalo, J. Wettability conversion on the liquid flame spray generated superhydrophobic TiO_2 nanoparticle coating on paper and board by photocatalytic decomposition of spontaneously accumulated carbonaceous overlayer. *Cellulose* **2013**, *20*, 391. [CrossRef]
74. Hwang, J.Y.; Kim, D.; Jang, H.; Lee, S.-Y.; Joo, Y.-C. Thermal and Electrical Properties Depending on the Bonding Structure of Amorphous Carbon Thin Films. *Electron. Mater. Lett.* **2024**, *20*, 648–656. [CrossRef]
75. Kim, J.W.; An, J.G.; Oh, G.H.; Park, J.H.; Kim, T. Improved Performance of Transparent MoS2 Thin-Film Transistor with IZO Electrodes by Air Thermal Annealing. *Electron. Mater. Lett.* **2024**, *20*, 225. [CrossRef]
76. O'Connor, B.T.; Reid, O.G.; Zhang, X.; Kline, R.J.; Richter, L.J.; Gundlach, D.J.; DeLongchamp, D.M.; Toney, M.F.; Kopidakis, N.; Rumbles, G. Morphological Origin of Charge Transport Anisotropy in Aligned Polythiophene Thin Films. *Adv. Funct. Mater.* **2014**, *24*, 3422. [CrossRef]
77. Du, C.; Wang, W.C.; Li, L.Q.; Fuchs, H.; Chi, L.F. Growth of rubrene crystalline thin films using thermal annealing on DPPC LB monolayer. *Org. Electron.* **2013**, *14*, 2534. [CrossRef]
78. Li, Y.; Sonar, P.; Singh, S.P.; Soh, M.S.; van Meurs, M.; Tan, J. Annealing-Free High-Mobility Diketopyrrolopyrrole−Quaterthiophene Copolymer for Solution-Processed Organic Thin Film Transistors. *J. Am. Chem. Soc.* **2011**, *133*, 2198. [CrossRef]
79. Shin, J.; Hong, T.R.; Lee, T.W.; Kim, A.; Kim, Y.H.; Cho, M.J.; Choi, D.H. Template-Guided Solution-Shearing Method for Enhanced Charge Carrier Mobility in Diketopyrrolopyrrole-Based Polymer Field-Effect Transistors. *Adv. Mater.* **2014**, *26*, 6031. [CrossRef]
80. Chen, H.; Guo, Y.; Yu, G.; Zhao, Y.; Zhang, J.; Gao, D.; Liu, H.; Liu, Y. Highly π-Extended Copolymers with Diketopyrrolopyrrole Moieties for High-Performance Field-Effect Transistors. *Adv. Mater.* **2012**, *24*, 4618. [CrossRef]
81. Yun, H.-J.; Kang, S.-J.; Xu, Y.; Kim, S.O.; Kim, Y.-H.; Noh, Y.-Y.; Kwon, S.-K. Dramatic Inversion of Charge Polarity in Diketopyrrolopyrrole-Based Organic Field-Effect Transistors via a Simple Nitrile Group Substitution. *Adv. Mater.* **2014**, *26*, 7300. [CrossRef] [PubMed]
82. Chen, J.H.; Tee, C.K.; Yang, J.Y.; Shaw, C.; Shtein, M.; Anthony, J.; Martin, D.C. Thermal and mechanical cracking in bis(triisopropylsilyiethnyl) pentacene thin films. *J. Polym. Sci. Part B-Polym. Phys.* **2006**, *44*, 3631. [CrossRef]
83. He, Z.; Li, D.; Hensley, D.K.; Rondinone, A.J.; Chen, J. Switching phase separation mode by varying the hydrophobicity of polymer additives in solution-processed semiconducting small-molecule/polymer blends. *Appl. Phys. Lett.* **2013**, *103*, 113301. [CrossRef]
84. He, Z.; Chen, J.; Sun, Z.; Szulczewski, G.; Li, D. Air-flow navigated crystal growth for TIPS pentacene-based organic thin-film transistors. *Org. Electron.* **2012**, *13*, 1819. [CrossRef]
85. He, Z.; Xiao, K.; Durant, W.; Hensley, D.K.; Anthony, J.E.; Hong, K.; Kilbey, S.M., II; Chen, J.; Li, D. Enhanced Performance Consistency in Nanoparticle/TIPS Pentacene-Based Organic Thin Film Transistors. *Adv. Funct. Mater.* **2011**, *21*, 3617. [CrossRef]
86. Diao, Y.; Tee, B.C.K.; Giri, G.; Xu, J.; Kim, D.H.; Becerril, H.A.; Stoltenberg, R.M.; Lee, T.H.; Xue, G.; Mannsfeld, S.C.B.; et al. Solution coating of large-area organic semiconductor thin films with aligned single-crystalline domains. *Nat. Mater.* **2013**, *12*, 665. [CrossRef] [PubMed]
87. Yuan, Y.B.; Giri, G.; Ayzner, A.L.; Zoombelt, A.P.; Mannsfeld, S.C.B.; Chen, J.H.; Nordlund, D.; Toney, M.F.; Huang, J.S.; Bao, Z.N. Ultra-high mobility transparent organic thin film transistors grown by an off-centre spin-coating method. *Nat. Commun.* **2014**, *5*, 3005. [CrossRef] [PubMed]
88. Zhang, Z.; Asare-Yeboah, K.; Bi, S.; He, Z. Poly(α-methyl styrene) polymer additive for organic thin film transistors. *J. Mater. Sci. Mater. Electron.* **2022**, *33*, 1101. [CrossRef]
89. He, Z.; Zhang, Z.; Asare-Yeboah, K.; Bi, S. Solvent Exchange in Controlling Semiconductor Morphology. *Electron. Mater. Lett.* **2022**, *18*, 501. [CrossRef]
90. Coropceanu, V.; Cornil, J.; da Silva Filho, D.A.; Olivier, Y.; Silbey, R.; Brédas, J.-L. Charge Transport in Organic Semiconductors. *Chem. Rev.* **2007**, *107*, 926. [CrossRef]
91. He, Z.; Zhang, Z.; Bi, S. Nanoparticles for organic electronics applications. *Mater. Res. Express* **2020**, *7*, 012004. [CrossRef]
92. Bronstein, H.; Nielsen, C.B.; Schroeder, B.C.; McCulloch, I. The role of chemical design in the performance of organic semiconductors. *Nat. Rev. Chem.* **2020**, *4*, 66. [CrossRef] [PubMed]
93. He, Z.; Zhang, Z.; Bi, S. Tailoring the molecular weight of polymer additives for organic semiconductors. *Mater. Adv.* **2022**, *3*, 1953. [CrossRef]

94. Virkar, A.A.; Mannsfeld, S.; Bao, Z.; Stingelin, N. Organic Semiconductor Growth and Morphology Considerations for Organic Thin-Film Transistors. *Adv. Mater.* **2010**, *22*, 3857. [CrossRef] [PubMed]
95. He, Z.; Chen, J.; Li, D. Polymer Additive Controlled Morphology for High Performance Organic Thin Film Transistors. *Soft Matter* **2019**, *15*, 5790. [CrossRef] [PubMed]
96. Wang, C.; Dong, H.; Jiang, L.; Hu, W. Organic semiconductor crystals. *Chem. Soc. Rev.* **2018**, *47*, 422. [CrossRef]
97. Yue, H.; Guo, M.; Ming, S.; Du, H.; Zhao, J.; Zhang, J. Fine-tuning the color hue of the solution-processable electrochromic copolymers based on the diketopyrrolopyrrole, benzodithiophene and dithienosilole units. *Colloids Surf. A Physicochem. Eng. Asp.* **2024**, *684*, 133094. [CrossRef]
98. Jiang, W.; Liu, Z.; Zhu, D.; Zheng, W.; Chen, L.; Zhang, X.; Zhang, G.; Yi, Y.; Jiang, L.; Zhang, D. New Synthetic Approaches to N-Aryl and π-Expanded Diketopyrrolopyrroles as New Building Blocks for Organic Optoelectronic Materials. *Angew. Chem. Int. Ed.* **2021**, *60*, 10700. [CrossRef]
99. Leenaers, P.J.; van Eersel, H.; Li, J.; Wienk, M.M.; Janssen, R.A.J. Influence of Regioregularity on the Optoelectronic Properties of Conjugated Diketopyrrolopyrrole Polymers Comprising Asymmetric Monomers. *Macromolecules* **2020**, *53*, 7749. [CrossRef]
100. Shen, T.; Wu, Z.; Jiang, Z.; Yan, D.; Zhao, Y.; Wang, Y.; Liu, Y. Elucidating the effects of the sidechain substitution direction on the optoelectronic properties of isomeric diketopyrrolopyrrole-based conjugated polymers for near-infrared organic phototransistors. *J. Mater. Chem. C* **2024**, *12*, 489. [CrossRef]
101. Adnan, M.; Kashif, M.; Irshad, Z.; Hussain, R.; Darwish, H.W.; Lim, J. Advancing optoelectronic characteristics of Diketopyrrolopyrrole-Based molecules as donors for organic and as hole transporting materials for perovskite solar cells. *Spectrochim. Acta Part A Mol. Biomol. Spectrosc.* **2024**, *320*, 124615. [CrossRef] [PubMed]
102. Farnum, D.G.; Mehta, G.; Moore, G.G.I.; Siegal, F.P. Attempted reformatskii reaction of benzonitrile, 1,4-diketo-3,6-diphenylpyrrolo [3,4-C]pyrrole. A lactam analogue of pentalene. *Tetrahedron Lett.* **1974**, *15*, 2549. [CrossRef]
103. Iqbal, A.; Jost, M.; Kirchmayr, R.; Pfenninger, J.; Rochat, A.; Wallquist, O. The synthesis and properties of 1,4-diketo-pyrrolo [3,4-C]pyrroles. *Bull. Sociétés Chim. Belg.* **1988**, *97*, 615. [CrossRef]
104. Yiu, A.T.; Beaujuge, P.M.; Lee, O.P.; Woo, C.H.; Toney, M.F.; Fréchet, J.M.J. Side-Chain Tunability of Furan-Containing Low-Band-Gap Polymers Provides Control of Structural Order in Efficient Solar Cells. *J. Am. Chem. Soc.* **2012**, *134*, 2180. [CrossRef]
105. Shaikh, S.A.L.; Birajdar, S.S.; Ambore, S.D.; Puyad, A.L.; Vijayanand, P.; Bhosale, S.V.; Bhosale, S.V. A minireview on diketopyrrolopyrrole chemistry: Historical perspective and recent developments. *Results Chem.* **2022**, *4*, 100473. [CrossRef]
106. Luo, N.; Zhang, G.; Liu, Z. Keep glowing and going: Recent progress in diketopyrrolopyrrole synthesis towards organic optoelectronic materials. *Org. Chem. Front.* **2021**, *8*, 4560. [CrossRef]
107. Tang, M.; Wu, S.; Xing, W.; Shen, H.; Xiang, L.; Liang, Y.; Xu, W.; Zhu, D. Diketopyrrolopyrrole based small molecular semiconductors containing thiazole units for solution-processed n-channel thin-film transistors. *Dyes Pigments* **2019**, *163*, 707. [CrossRef]
108. Kwon, J.-H.; Kim, M.-H.; Bae, J.-H. A review on diverse streams of interface engineering for organic thin-film transistors. *J. Mater. Chem. C* **2024**, *12*, 29. [CrossRef]
109. Song, J.; Liu, H.; Zhao, Z.; Lin, P.; Yan, F. Flexible Organic Transistors for Biosensing: Devices and Applications. *Adv. Mater.* **2024**, *36*, 2300034. [CrossRef]
110. Shin, H.; Kim, D.; Park, J.; Kim, D.Y. Improving Photosensitivity and Transparency in Organic Phototransistor with Blending Insulating Polymers. *Micromachines* **2023**, *14*, 620. [CrossRef]
111. Jain, S.K.; Joshi, A.M.; Bharti, D. Effect of Temperature on Performance Characteristics with Varying Defect States Parameters in TIPS-pentacene Based OTFTs on n++ Silicon Substrate. *Silicon* **2023**, *15*, 6397. [CrossRef]
112. He, Z.; Chen, J.; Keum, J.K.; Szulczewski, G.; Li, D. Improving performance of TIPS pentacene-based organic thin film transistors with small-molecule additives. *Org. Electron.* **2014**, *15*, 150. [CrossRef]
113. Chen, J.; Shao, M.; Xiao, K.; He, Z.; Li, D.; Lokitz, B.S.; Hensley, D.K.; Kilbey, S.M., II; Anthony, J.E.; Keum, J.K.; et al. Conjugated Polymer-Mediated Polymorphism of a High Performance, Small-Molecule Organic Semiconductor with Tuned Intermolecular Interactions, Enhanced Long-Range Order, and Charge Transport. *Chem. Mater.* **2013**, *25*, 4378. [CrossRef]
114. Lewińska, G. Ternary Organic Solar Cells—Simulation–Optimization Approach. *Electron. Mater. Lett.* **2024**, *20*, 440. [CrossRef]
115. Corzo, D.; Rosas-Villalva, D.; C, A.; Tostado-Blázquez, G.; Alexandre, E.B.; Hernandez, L.H.; Han, J.; Xu, H.; Babics, M.; De Wolf, S.; et al. High-performing organic electronics using terpene green solvents from renewable feedstocks. *Nat. Energy* **2023**, *8*, 62. [CrossRef]
116. Ayub, A.; Ans, M.; Gul, S.; Shawky, A.M.; Ayub, K.; Iqbal, J.; Hashmi, M.A.; Lakhani, A. Toward High-Performance Quinoxaline Based Non-fullerene Small Molecule Acceptors for Organic Solar Cells. *Electron. Mater. Lett.* **2023**, *19*, 38. [CrossRef]
117. Xu, X.; Zhao, Y.; Liu, Y. Wearable Electronics Based on Stretchable Organic Semiconductors. *Small* **2023**, *19*, 2206309. [CrossRef]
118. Aderne, R.E.; Borges, B.G.A.L.; Ávila, H.C.; von Kieseritzky, F.; Hellberg, J.; Koehler, M.; Cremona, M.; Roman, L.S.; Araujo, C.M.; Rocco, M.L.M.; et al. On the energy gap determination of organic optoelectronic materials: The case of porphyrin derivatives. *Mater. Adv.* **2022**, *3*, 1791. [CrossRef]
119. Sani, M.J. Theoretical survey on the electronic, linear and nonlinear optical properties of substituted benzenes and polycondensed π-systems. A density functional theory study. *Comput. Theor. Chem.* **2023**, *1223*, 114100. [CrossRef]
120. Huang, J.; Yu, G. Recent progress in quinoidal semiconducting polymers: Structural evolution and insight. *Mater. Chem. Front.* **2021**, *5*, 76. [CrossRef]

121. Liu, Q.; Bottle, S.E.; Sonar, P. Developments of Diketopyrrolopyrrole-Dye-Based Organic Semiconductors for a Wide Range of Applications in Electronics. *Adv. Mater.* **2020**, *32*, 1903882. [CrossRef] [PubMed]
122. Grzybowski, M.; Gryko, D.T. Diketopyrrolopyrroles: Synthesis, Reactivity, and Optical Properties. *Adv. Opt. Mater.* **2015**, *3*, 280. [CrossRef]
123. Addanki Tirumala, R.T.; Khatri, N.; Ramakrishnan, S.B.; Mohammadparast, F.; Khan, M.T.; Tan, S.; Wagle, P.; Puri, S.; McIlroy, D.N.; Kalkan, A.K.; et al. Tuning Catalytic Activity and Selectivity in Photocatalysis on Mie-Resonant Cuprous Oxide Particles: Distinguishing Electromagnetic Field Enhancement Effect from the Heating Effect. *ACS Sustain. Chem. Eng.* **2023**, *11*, 15931. [CrossRef]
124. Tirumala, R.T.A.; Gyawali, S.; Wheeler, A.; Ramakrishnan, S.B.; Sooriyagoda, R.; Mohammadparast, F.; Khatri, N.; Tan, S.; Kalkan, A.K.; Bristow, A.D.; et al. Structure–Property–Performance Relationships of Cuprous Oxide Nanostructures for Dielectric Mie Resonance-Enhanced Photocatalysis. *ACS Catal.* **2022**, *12*, 7975. [CrossRef]
125. Gyawali, S.; Tirumala, R.T.A.; Andiappan, M.; Bristow, A.D. Size- and Shape-Dependent Charge-Carrier Dynamics in Sub-micron Cuprous Oxide Nanoparticles. In Proceedings of the Frontiers in Optics + Laser Science 2022 (FIO, LS), Rochester, NY, USA, 16–20 October 2022, (*unpublished*).
126. Yu, Y.-Y.; Chien, W.-C.; Wang, Y.-J. Copper oxide hole transport materials for heterojunction solar cell applications. *Thin Solid Films* **2016**, *618*, 134. [CrossRef]
127. Meng, D.; Zheng, R.; Zhao, Y.; Zhang, E.; Dou, L.; Yang, Y. Near-Infrared Materials: The Turning Point of Organic Photovoltaics. *Adv. Mater.* **2022**, *34*, 2107330. [CrossRef]
128. Zhao, Z.; Xu, C.; Niu, L.; Zhang, X.; Zhang, F. Recent Progress on Broadband Organic Photodetectors and their Applications. *Laser Photonics Rev.* **2020**, *14*, 2000262. [CrossRef]
129. Tong, G.; Jiang, M.; Son, D.-Y.; Qiu, L.; Liu, Z.; Ono, L.K.; Qi, Y. Inverse Growth of Large Grain Size and Stable Inorganic Perovskite Micro-Nanowire Photodetectors. *ACS Appl. Mater. Interfaces* **2020**, *12*, 14185. [CrossRef] [PubMed]
130. Zhang, Y.P.; Deng, W.; Zhang, X.J.; Zhang, X.W.; Zhang, X.H.; Xing, Y.L.; Jie, J.S. In Situ Integration of Squaraine-Nanowire-Array-Based Schottky-Type Photodetectors with Enhanced Switching Performance. *ACS Appl. Mater. Interfaces* **2013**, *5*, 12288. [CrossRef]
131. Qian, G.; Qi, J.; Wang, Z.Y. Synthesis and study of low-bandgap polymers containing the diazapentalene and diketopyrrolopyrrole chromophores for potential use in solar cells and near-infrared photodetectors. *J. Mater. Chem.* **2012**, *22*, 12867. [CrossRef]
132. Kwon, J.H.; Shin, S.I.; Kim, C.H.; You, I.K.; Cho, C.I.; Ju, B.K. Flexible Organic Thin-film Transistors for Photodetectors. *J. Korean Phys. Soc.* **2009**, *55*, 72. [CrossRef]
133. Bassous, N.J.; Rodriguez, A.C.; Leal, C.I.L.; Jung, H.Y.; Lee, C.K.; Joo, S.; Kim, S.; Yun, C.; Hahm, M.G.; Ahn, M.-H.; et al. Significance of Various Sensing Mechanisms for Detecting Local and Atmospheric Greenhouse Gases: A Review. *Adv. Sens. Res.* **2024**, *3*, 2300094. [CrossRef]
134. Suh, J.M.; Eom, T.H.; Cho, S.H.; Kim, T.; Jang, H.W. Light-activated gas sensing: A perspective of integration with micro-LEDs and plasmonic nanoparticles. *Mater. Adv.* **2021**, *2*, 827. [CrossRef]
135. Pan, Y.; Yu, G. Multicomponent Blend Systems Used in Organic Field-Effect Transistors: Charge Transport Properties, Large-Area Preparation, and Functional Devices. *Chem. Mater.* **2021**, *33*, 2229. [CrossRef]
136. Cavallari, M.R.; Pastrana, L.M.; Sosa, C.D.; Marquina, A.M.; Izquierdo, J.E.; Fonseca, F.J.; Amorim, C.A.; Paterno, L.G.; Kymissis, I. Organic Thin-Film Transistors as Gas Sensors: A Review. *Materials* **2021**, *14*, 3. [CrossRef]
137. Addanki Tirumala, R.T.; Ramakrishnan, S.B.; Mohammadparast, F.; Khatri, N.; Arumugam, S.M.; Tan, S.; Kalkan, A.K.; Andiappan, M. Structure–Property–Performance Relationships of Dielectric Cu_2O Nanoparticles for Mie Resonance-Enhanced Dye Sensitization. *ACS Appl. Nano Mater.* **2022**, *5*, 6699. [CrossRef]
138. Gyawali, S.; Tirumala, R.T.A.; Loh, H.; Andiappan, M.; Bristow, A.D. Photocarrier Recombination Dynamics in Highly Scattering Cu_2O Nanocatalyst Clusters. *J. Phys. Chem. C* **2024**, *128*, 2003. [CrossRef]
139. Peng, S.-H.; Huang, T.-W.; Gollavelli, G.; Hsu, C.-S. Thiophene and diketopyrrolopyrrole based conjugated polymers as efficient alternatives to spiro-OMeTAD in perovskite solar cells as hole transporting layers. *J. Mater. Chem. C* **2017**, *5*, 5193. [CrossRef]
140. Li, Y.N.; Sonar, P.; Murphy, L.; Hong, W. High mobility diketopyrrolopyrrole (DPP)-based organic semiconductor materials for organic thin film transistors and photovoltaics. *Energy Environ. Sci.* **2013**, *6*, 1684. [CrossRef]
141. Otep, S.; Lin, Y.-C.; Matsumoto, H.; Mori, T.; Wei, K.-H.; Michinobu, T. Diketopyrrolopyrrole–thiophene–methoxythiophene based random copolymers for organic field effect transistor applications. *Org. Electron.* **2020**, *87*, 105986. [CrossRef]
142. Chen, J.; Zhou, J.; Li, N.; Ding, Y.; Ren, S.; Zeng, M. Novel Divinyl-Flanked Diketopyrrolopyrrole Polymer, Based on a Dimerization Strategy for High-Performance Organic Field-Effect Transistors. *Polymers* **2023**, *15*, 4546. [CrossRef]
143. Bürgi, L.; Turbiez, M.; Pfeiffer, R.; Bienewald, F.; Kirner, H.-J.; Winnewisser, C. High-Mobility Ambipolar Near-Infrared Light-Emitting Polymer Field-Effect Transistors. *Adv. Mater.* **2008**, *20*, 2217. [CrossRef]
144. Bi, S.; He, Z.; Chen, J.; Li, D. Solution-grown small-molecule organic semiconductor with enhanced crystal alignment and areal coverage for organic thin film transistors. *AIP Adv.* **2015**, *5*, 077170. [CrossRef]
145. Bi, S.; Li, Y.; He, Z.; Ouyang, Z.; Guo, Q.; Jiang, C. Self-assembly diketopyrrolopyrrole-based materials and polymer blend with enhanced crystal alignment and property for organic field-effect transistors. *Org. Electron.* **2019**, *65*, 96. [CrossRef]

146. Chen, Z.; Lee, M.J.; Shahid Ashraf, R.; Gu, Y.; Albert-Seifried, S.; Meedom Nielsen, M.; Schroeder, B.; Anthopoulos, T.D.; Heeney, M.; McCulloch, I.; et al. High-Performance Ambipolar Diketopyrrolopyrrole-Thieno [3,2-b]thiophene Copolymer Field-Effect Transistors with Balanced Hole and Electron Mobilities. *Adv. Mater.* **2012**, *24*, 647. [CrossRef] [PubMed]
147. Nelson, T.L.; Young, T.M.; Liu, J.; Mishra, S.P.; Belot, J.A.; Balliet, C.L.; Javier, A.E.; Kowalewski, T.; McCullough, R.D. Transistor Paint: High Mobilities in Small Bandgap Polymer Semiconductor Based on the Strong Acceptor, Diketopyrrolopyrrole and Strong Donor, Dithienopyrrole. *Adv. Mater.* **2010**, *22*, 4617. [CrossRef]
148. Sonar, P.; Singh, S.P.; Li, Y.; Soh, M.S.; Dodabalapur, A. A Low-Bandgap Diketopyrrolopyrrole-Benzothiadiazole-Based Copolymer for High-Mobility Ambipolar Organic Thin-Film Transistors. *Adv. Mater.* **2010**, *22*, 5409. [CrossRef]
149. Shahid, M.; McCarthy-Ward, T.; Labram, J.; Rossbauer, S.; Domingo, E.B.; Watkins, S.E.; Stingelin, N.; Anthopoulos, T.D.; Heeney, M. Low band gap selenophene–diketopyrrolopyrrole polymers exhibiting high and balanced ambipolar performance in bottom-gate transistors. *Chem. Sci.* **2012**, *3*, 181. [CrossRef]
150. Shin, J.; Park, G.E.; Lee, D.H.; Um, H.A.; Lee, T.W.; Cho, M.J.; Choi, D.H. Bis(thienothiophenyl) Diketopyrrolopyrrole-Based Conjugated Polymers with Various Branched Alkyl Side Chains and Their Applications in Thin-Film Transistors and Polymer Solar Cells. *ACS Appl. Mater. Interfaces* **2015**, *7*, 3280. [CrossRef]
151. Kanimozhi, C.; Yaacobi-Gross, N.; Chou, K.W.; Amassian, A.; Anthopoulos, T.D.; Patil, S. Diketopyrrolopyrrole–Diketopyrrolopyrrole-Based Conjugated Copolymer for High-Mobility Organic Field-Effect Transistors. *J. Am. Chem. Soc.* **2012**, *134*, 16532. [CrossRef]
152. Bronstein, H.; Chen, Z.; Ashraf, R.S.; Zhang, W.; Du, J.; Durrant, J.R.; Shakya Tuladhar, P.; Song, K.; Watkins, S.E.; Geerts, Y.; et al. Thieno [3,2-b]thiophene−Diketopyrrolopyrrole-Containing Polymers for High-Performance Organic Field-Effect Transistors and Organic Photovoltaic Devices. *J. Am. Chem. Soc.* **2011**, *133*, 3272. [CrossRef] [PubMed]
153. Wang, B.; Huynh, T.-P.; Wu, W.; Hayek, N.; Do, T.T.; Cancilla, J.C.; Torrecilla, J.S.; Nahid, M.M.; Colwell, J.M.; Gazit, O.M.; et al. A Highly Sensitive Diketopyrrolopyrrole-Based Ambipolar Transistor for Selective Detection and Discrimination of Xylene Isomers. *Adv. Mater.* **2016**, *28*, 4012. [CrossRef]
154. Nikolka, M.; Nasrallah, I.; Rose, B.; Ravva, M.K.; Broch, K.; Sadhanala, A.; Harkin, D.; Charmet, J.; Hurhangee, M.; Brown, A.; et al. High operational and environmental stability of high-mobility conjugated polymer field-effect transistors through the use of molecular additives. *Nat. Mater.* **2017**, *16*, 356. [CrossRef] [PubMed]
155. Onojima, N.; Akiyama, N.; Mori, Y.; Sugai, T.; Obata, S. Small molecule/polymer blends prepared by environmentally-friendly process for mechanically-stable flexible organic field-effect transistors. *Org. Electron.* **2020**, *78*, 105597. [CrossRef]
156. Bharti, D.; Tiwari, S.P. Crystallinity and performance improvement in solution processed organic field-effect transistors due to structural dissimilarity of the additive solvent. *Synth. Met.* **2016**, *215*, 1. [CrossRef]
157. Chae, G.J.; Jeong, S.H.; Baek, J.H.; Walker, B.; Song, C.K.; Seo, J.H. Improved performance in TIPS-pentacene field effect transistors using solvent additives. *J. Mater. Chem. C* **2013**, *1*, 4216. [CrossRef]
158. Park, Y.J.; Seo, J.H.; Elsawy, W.; Walker, B.; Cho, S.; Lee, J.S. Enhanced performance in isoindigo based organic small molecule field-effect transistors through solvent additives. *J. Mater. Chem. C* **2015**, *3*, 5951. [CrossRef]
159. Yamazaki, S.; Hamada, T.; Nagase, T.; Tokai, S.; Yoshikawa, M.; Kobayashi, T.; Michiwaki, Y.; Watase, S.; Watanabe, M.; Matsukawa, K.; et al. Drastic Improvement in Wettability of 6,13-Bis(triisopropylsilylethynyl)pentacene by Addition of Silica Nanoparticles for Solution-Processable Organic Field-Effect Transistors. *Appl. Phys. Express* **2010**, *3*, 091602. [CrossRef]
160. Afsharimani, N.; Nysten, B. Hybrid gate dielectrics: A comparative study between polyvinyl alcohol/SiO2 nanocomposite and pure polyvinyl alcohol thin-film transistors. *Bull. Mater. Sci.* **2019**, *42*, 0026. [CrossRef]
161. Nagase, T.; Yoshikawa, M.; Yamazaki, S.; Kobayashi, T.; Michiwaki, Y.; Watase, S.; Watanabe, M.; Matsukawa, K.; Naito, H. Effects of Silica Nanoparticle Addition on Polymer Semiconductor Wettability and Carrier Mobility in Solution-Processable Organic Transistors on Hydrophobic Substrates. *J. Polym. Sci. Part B-Polym. Phys.* **2016**, *54*, 509. [CrossRef]
162. Wang, X.S.; Wang, H.; Li, Y.; Shi, Z.S.; Yan, D.H.; Cui, Z.C. Polymer/Silicon Nanoparticle Hybrid Layer as High-k Dielectrics in Organic Thin-Film Transistors. *J. Phys. Chem. C* **2018**, *122*, 11214. [CrossRef]
163. Jang, Y.; Lee, W.H.; Park, Y.D.; Kwak, D.; Cho, J.H.; Cho, K. High field-effect mobility pentacene thin-film transistors with nanoparticle polymer composite/polymer bilayer insulators. *Appl. Phys. Lett.* **2009**, *94*, 183301. [CrossRef]
164. Wang, S.M.; Leung, C.W.; Chan, P.K.L. Nonvolatile organic transistor-memory devices using various thicknesses of silver nanoparticle layers. *Appl. Phys. Lett.* **2010**, *97*, 023511. [CrossRef]
165. Ryu, S.; Yun, C.; Ryu, S.; Ahn, J.; Kim, C.; Seo, S. Recent Progress in Perovskite Solar Cells: Status and Future. *Coatings* **2023**, *13*, 644. [CrossRef]
166. Suzuki, I.; Hanna, J.-I.; Iino, H. High-speed blade-coating using liquid crystalline organic semiconductor Ph-BTBT-10. *Appl. Phys. Express* **2024**, *17*, 051007. [CrossRef]
167. Hodsden, T.; Thorley, K.J.; Basu, A.; White, A.J.P.; Wang, C.; Mitchell, W.; Glöcklhofer, F.; Anthopoulos, T.D.; Heeney, M. The influence of alkyl group regiochemistry and backbone fluorination on the packing and transistor performance of N-cyanoimine functionalised indacenodithiophenes. *Mater. Adv.* **2021**, *2*, 1706. [CrossRef]
168. Fo, W.-Z.; Xu, G.Y.; Dong, H.-J.; Liu, L.-N.; Li, Y.W.; Ding, L. Highly Efficient Binary Solvent Additive-Processed Organic Solar Cells by the Blade-Coating Method. *Macromol. Chem. Phys.* **2021**, *222*, 2100062. [CrossRef]
169. Ouyang, Z.; Yang, M.; Whitaker, J.B.; Li, D.; van Hest, M.F. Toward Scalable Perovskite Solar Modules Using Blade Coating and Rapid Thermal Processing. *ACS Appl. Energy Mater.* **2020**, *3*, 3714. [CrossRef]

170. Chen, M.; Peng, B.; Huang, S.; Chan, P.K.L. Understanding the Meniscus-Guided Coating Parameters in Organic Field-Effect-Transistor Fabrications. *Adv. Funct. Mater.* **2020**, *30*, 1905963. [CrossRef]
171. Pierre, A.; Sadeghi, M.; Payne, M.M.; Facchetti, A.; Anthony, J.E.; Arias, A.C. All-Printed Flexible Organic Transistors Enabled by Surface Tension-Guided Blade Coating. *Adv. Mater.* **2014**, *26*, 5722. [CrossRef]
172. Lee, W.H.; Park, Y.D. Organic Semiconductor/Insulator Polymer Blends for High-Performance Organic Transistors. *Polymers* **2014**, *6*, 1057. [CrossRef]
173. Suzuki, T.; De Nicola, A.; Okada, T.; Matsui, H. Fully Atomistic Molecular Dynamics Simulation of a TIPS-Pentacene:Polystyrene Mixed Film Obtained via the Solution Process. *Nanomaterials* **2023**, *13*, 312. [CrossRef] [PubMed]
174. Raghuwanshi, V.; Bharti, D.; Mahato, A.K.; Varun, I.; Tiwari, S.P. Solution-processed organic field-effect transistors with high performance and stability on paper substrates. *ACS Appl. Mater. Interfaces* **2019**, *11*, 8357. [CrossRef]
175. Lin, Z.; Guo, X.; Zhou, L.; Zhang, C.; Chang, J.; Wu, J.; Zhang, J. Solution-processed high performance organic thin film transistors enabled by roll-to-roll slot die coating technique. *Org. Electron.* **2018**, *54*, 80. [CrossRef]
176. Feng, L.; Jiang, C.; Ma, H.; Guo, X.; Nathan, A. All ink-jet printed low-voltage organic field-effect transistors on flexible substrate. *Org. Electron.* **2016**, *38*, 186. [CrossRef]
177. Huang, Z.-T.; Xue, G.-B.; Wu, J.-K.; Liu, S.; Li, H.-B.; Yang, Y.-H.; Yan, F.; Chan, P.K.L.; Chen, H.-Z.; Li, H.-Y. Electron transport in solution-grown TIPS-pentacene single crystals: Effects of gate dielectrics and polar impurities. *Chin. Chem. Lett.* **2016**, *27*, 1781. [CrossRef]
178. Bharti, D.; Tiwari, S.P. Phase separation induced high mobility and electrical stability in organic field-effect transistors. *Synth. Met.* **2016**, *221*, 186. [CrossRef]